


# **The 30 December 2021 Colorado Front Range Windstorm and Marshall Fire: Evolution of Surface and 3D Structure, NWP Guidance, NWS Forecasts, and Decision Support**

STANLEY G. BENJAMIN<sup>a,b</sup>, ERIC P. JAMES,<sup>a,b</sup> EDWARD J. SZOKE,<sup>c,b</sup> PAUL T. SCHLATTER,<sup>d</sup> AND JOHN M. BROWN<sup>b</sup>

<sup>a</sup> CIRES, University of Colorado Boulder, Boulder, Colorado

<sup>b</sup> NOAA/Global Systems Laboratory, Boulder, Colorado

<sup>c</sup> CIRA, Colorado State University, Fort Collins, Colorado

<sup>d</sup> National Weather Service, Boulder, Colorado

(Manuscript received 24 May 2023, in final form 15 September 2023, accepted 18 September 2023)

**ABSTRACT:** The Marshall Fire on 30 December 2021 became the most destructive wildfire costwise in Colorado history as it evolved into a suburban firestorm in southeastern Boulder County, driven by strong winds and a snow-free and drought-influenced fuel state. The fire was driven by a strong downslope windstorm that maintained its intensity for nearly 11 hours. The southward movement of a large-scale jet axis across Boulder County brought a quick transition that day into a zone of upper-level descent, enhancing the midlevel inversion providing a favorable environment for an amplifying downstream mountain wave. In several aspects, this windstorm did not follow typical downslope windstorm behavior. NOAA rapidly updating numerical weather prediction guidance (including the High-Resolution Rapid Refresh) provided operationally useful forecasts of the windstorm, leading to the issuance of a High-Wind Warning (HWW) for eastern Boulder County. No Red Flag Warning was issued due to a too restrictive relative humidity criterion (already published alternatives are recommended); however, owing to the HWW, a countywide burn ban was issued for that day. Consideration of spatial (vertical and horizontal) and temporal (both valid time and initialization time) neighborhoods allows some quantification of forecast uncertainty from deterministic forecasts—important in real-time use for forecasting and public warnings of extreme events. Essentially, dimensions of the deterministic model were used to roughly estimate an ensemble forecast. These dimensions including run-to-run consistency are also important for subsequent evaluation of forecasts for small-scale features such as downslope windstorms and the tropospheric features responsible for them, similar to forecasts of deep, moist convection and related severe weather.


**SIGNIFICANCE STATEMENT:** The Front Range windstorm of 30 December 2021 combined extreme surface winds ( $>45 \text{ m s}^{-1}$ ) with fire ignition resulting in an extraordinary and quickly evolving, extremely destructive wildfire–urban interface fire event. This windstorm differed from typical downslope windstorms in several aspects. We describe the observations, model guidance, and decision-making of operational forecasters for this event. In effect, an ensemble forecast was approximated by use of a frequently updated deterministic model by operational forecasters, and this combined use of temporal, spatial (horizontal and vertical), and other forecast dimensions is suggested to better estimate the possibility of such extreme events.

**KEYWORDS:** Downslope winds; Wildfires; Orographic effects; Operational forecasting; Emergency response; Wind effects

## **1. Introduction and outcome from event**

On 30 December 2021, a fast-moving wildfire driven by a strong downslope windstorm burned through  $24 \text{ km}^2$  of rural and suburban areas of southeast Boulder County, becoming Colorado's most destructive wildfire (costwise) to date (Boulder County Sheriff's Office 2023). The fire, named the Marshall Fire for its point of origin near Marshall, Colorado, led to the destruction of almost 1100 homes (e.g., Fig. 1; Boulder County 2022) and seven businesses, damage to numerous other homes and businesses, and overall damage of over \$2 billion (RMILA 2023). Tragically, two people were killed. Severe downslope

windstorms are a notable wintertime feature of the climate of the Boulder area (Sangster 1972). However, major fires during these wintertime downslope windstorms have been rare, and fire spreading substantially eastward from the foothills is also uncommon (Boulder County 2023). The Marshall Fire was unprecedented in these aspects and in its destruction, primary motivators for this study. While there were many factors that contributed to the rapid fire spread, the most important was the strength of the wind. An average of five events with wind gusts  $> 31.3 \text{ m s}^{-1}$  (70 mph or 60.9 kt) occurs per year at the NCAR Mesa Laboratory over a 53-yr record (NOAA Physical Science Laboratory 2023). These downslope windstorms, especially when combined with a fire ignition, are more impactful and consequently more challenging for operational weather prediction. The 30 December 2021 event was exceptional in combining two extreme aspects, wind gusts  $> 45 \text{ m s}^{-1}$  and a grass-urban fire, into a single event that day. The lack of any snowfall yet in that cold season (part of a multimonth drought since July) and dryness of high fine fuel loading in late December made

 Denotes content that is immediately available upon publication as open access.

Corresponding author: Stanley G. Benjamin, stan.benjamin@noaa.gov



FIG. 1. Scene from the Marshall Fire, near Harper Lake in Louisville, CO,  $\sim$ 1800 LT 30 Dec 2021. (From video by KCNC4, Denver.)

this a unique event in Colorado. An overview on surface and upper-air conditions for the 30 December 2021 event has been provided by Fovell et al. (2022). In this paper, we provide a merged perspective on climatological and meteorological conditions for both the windstorm and fire, and we also describe the performance of numerical weather prediction, particularly as it pertains to the human forecast and decision support services both provided by the local National Weather Service (NWS) Forecast Office in Boulder, Colorado.

As described in some detail in this paper, this downslope windstorm started along the Colorado Front Range at 0800–0900 local time (LT, equal to UTC  $- 7$  h) 30 December 2021 with the strongest winds from south Boulder southward for 20 km. The wind intensity increased during that morning and by 1100 LT, with observed gusts up to over  $45 \text{ m s}^{-1}$  (100 mph) at a few locations. Fires were initiated by 1108 LT (first smoke report via social media and 911 call logs, preceding an initial *GOES-16* hotspot indicator at 1131 LT), spreading rapidly downwind and causing destruction as they moved from grasslands into an urban, heavily populated area. Southwesterly to westerly wind gusts often greater than  $36 \text{ m s}^{-1}$  (roughly 80 mph) occurred over the next 8 h, finally weakening to less than  $25 \text{ m s}^{-1}$  by 1930 LT that evening.

#### a. Classic Boulder windstorm—3D and surface structure

Strong downslope winds on the lee side of mountain ranges are a notable feature of the climate in many parts of the world [Smith 2019, their section 4b(3)]. In North America, these are mainly a cold-season phenomenon and are observed frequently to the east of the Rocky Mountains at many locations from Alberta southward to New Mexico and with somewhat lower frequency to the east of the Cascade Range in Washington and Oregon and east of the Sierra Nevada in California. The Santa

Ana winds in southwest California are another example of downslope windstorms that not only can damage property but also may result in rapid fire spread given the state of the vegetation and dryness of the downslope flow.

Because of their distinctive properties (often being associated with dramatic temperature rises at onset, notable gustiness, and intermittency, and particularly their potential for damage to structures and vegetation), downslope windstorms have been extensively studied. An unintended consequence of the decision to locate the National Center for Atmospheric Research (NCAR) and certain research laboratories of NOAA in Boulder, Colorado, to the lee of the Colorado Front Range of the Rocky Mountains in the 1960s was a flowering of research stimulated by several windstorms that caused major structural damage in Boulder (Lilly 1978; Brinkmann 1973, 1974; Lilly and Zipser 1972). From this emerged an understanding of the dynamics of severe downslope windstorms that has now become generally accepted, summarized well by Durran (1990).

Figure 2 shows the results of idealized dry numerical simulations by Durran (1986) that illustrate an analogy between water flowing over a weir or dam and airflow over a two-dimensional ridge. Early on in the studies of Boulder windstorms, it was recognized that there is often a temperature inversion or stable layer near mountain-top level in rawinsonde observations (hereafter raobs) taken upstream of the Continental Divide in Colorado, most often from operational raobs launched from Grand Junction (KGJT). The simulations of Fig. 2 illustrate why this can be important, given sufficiently strong cross-mountain ambient flow at mountain-top level,  $\sim 10 \text{ m s}^{-1}$  or greater.

Figure 2a shows four stability configurations used by Durran (1986). All four two panels show a surface-based stable layer surmounted by lower static stability but with an interface at increasing height from 1000 to 4000 m. Because the flow is isentropic,

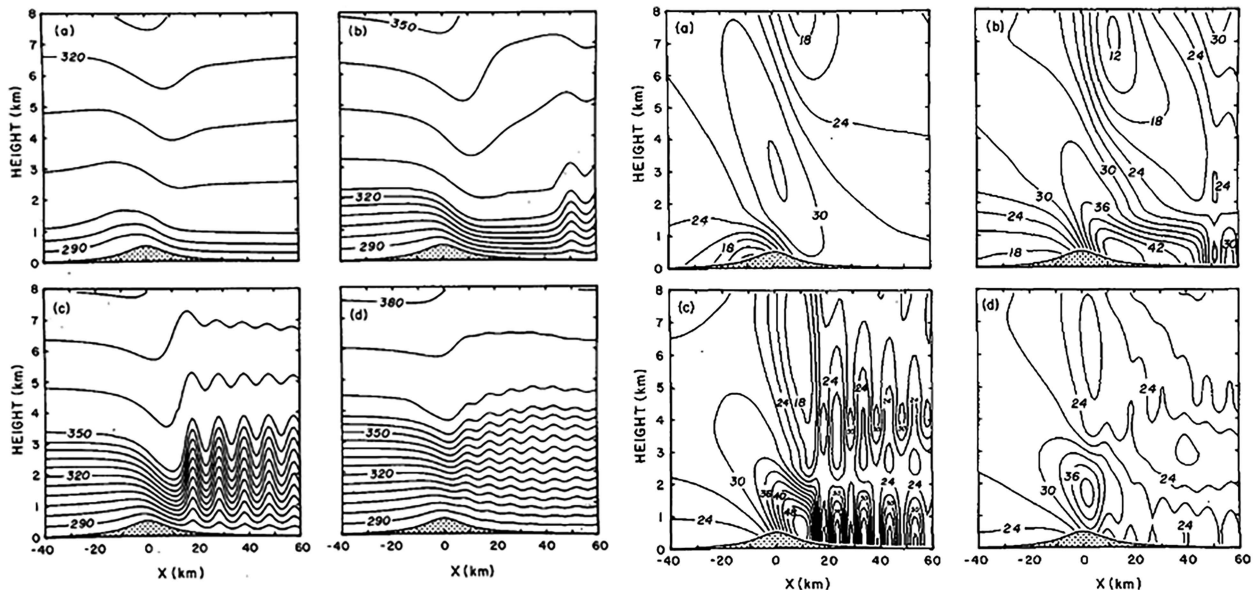


FIG. 2. Idealized mountain-wave simulations [from Durrán (1986), their Figs. 5 and 6] of (left) isentropes (K) and (right) horizontal wind speed ( $\text{m s}^{-1}$ ) for four different stability configurations. The solution is for a two-layer atmosphere flowing from left to right over a mountain (500 m) at a nondimensional time ( $U/la = 25$ , where  $a$  is the half-width of the mountain and  $U$  is the unperturbed upstream horizontal flow speed). Four different stability structures are shown all with surface-based high static stability surmounted by lower static stability and the interface between layers of different stability at increasing heights: (a) 1000, (b) 2500, (c) 3500, and (d) 4000 m.

vertical variations in the vertical distance between isentropes are correlated with vertical variations in the horizontal airflow, as can be seen by comparing the respective panels of Figs. 2a and 2b. (These experiments are without surface friction.)

It is apparent here that the vertical variation in stratification has a profound impact on the flow. For the cases with a shallow (1000 m) or very deep (4000 m) stable layer, the flow proceeds smoothly across the ridge and downstream with some acceleration down the lee slope. However, for the case with a 3500-m-deep stable layer based at the surface, the solution is radically different. The flow east of the ridge crest accelerates strongly down the lee slope, terminating abruptly in a hydraulic jump east of the ridge. We show evidence in sections 2 and 3 that in the 30 December 2021 case, there was in fact a strong hydraulic jump roughly 10–15 km east of the eastern edge of the foothills (although with a different stability profile than that shown by Durrán 1986) with very strong westerly flow westward (closer to the mountains) of the jump. As explained in Durrán (1986) and Durrán and Klemp (1983), this is the analogy between the atmospheric flow over the Front Range and water accelerating over and down the face of a dam and terminating in a turbulent hydraulic jump at its base. A similar process can also be seen in the flow of a shallow stream over a rocky stream bed as the flow becomes locally supercritical as it flows over larger rocks that are still submerged.

A typical 500-hPa pattern (Fig. 3) for a Boulder downslope windstorm (from Mercer et al. 2008) includes west-northwest-to-northwest ( $292^{\circ}$ – $315^{\circ}$ ) flow aloft over Colorado and most of the U.S. Northwest. This pattern corresponds to the warm-advection scenario (chinook) with high winds limited to within 10–20 km of the foothills. This chinook pattern with northwest

flow aloft was also evident for the classic 11 January 1972 Boulder windstorm (Lilly and Zipser 1972, their Fig. 3). Mercer et al. (2008) also showed classical synoptic patterns for cold-air advection (bora) with strong winds typically spreading over a much wider area, across much of northeastern Colorado. As discussed later, the 30 December 2021 case was neither a classic chinook nor a bora windstorm with atypical flow conditions.

### b. Overview of paper

In this paper, we examine the meteorological conditions that led to the severe windstorm on 30 December 2021 and determine

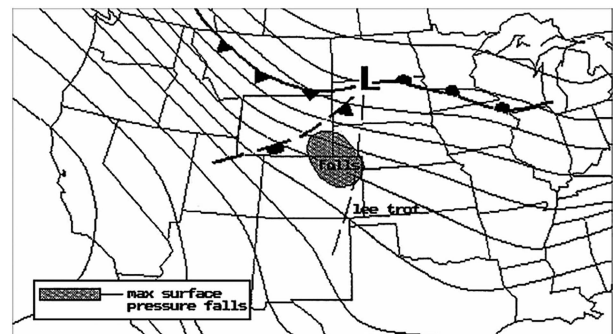


FIG. 3. Typical synoptic pattern (500 hPa, surface) associated with a “prefrontal” windstorm at Boulder (from Mercer et al. 2008): surface frontal positions are shown, along with the locations of the surface warm, cold, and Pacific occluded fronts. The shaded area labeled “falls” indicates the location of the largest 3-h falls in surface-station pressure, which typically has tracked eastward across southern WY. The typical position of a “lee trough” on the high plains is also indicated. Thin solid curved lines are 500-hPa height contours.



to what extent numerical weather prediction (NWP) guidance provided operationally useful forecast information in the days and hours leading up to the windstorm. Sections 2 and 3 discuss the meteorological setting: section 2 using near-surface observations and analyses and section 3 focusing on conditions aloft including aspects that make this case unique. In section 4, we present numerical model guidance, with a particular focus on the 3-km NOAA High-Resolution Rapid Refresh (HRRR) model (Dowell et al. 2022; James et al. 2022; Benjamin et al. 2016), illustrating how probabilistic information can be obtained from frequently updating deterministic models. Section 5 presents the operational forecast process for the event by the NWS Forecast Office in Boulder, particularly how high-resolution model guidance and fire-weather conditions are incorporated into the decision-making process. Finally, section 6 provides some conclusions about the case including recommendations on how to use NWP (e.g., ensemble components, run-to-run consistency, for cases like this one) and examines issues associated with Red Flag Warning criteria.

## 2. Evolution of the 30 December 2021 windstorm event at the surface

The 30 December 2021 windstorm event started at lower elevations around 0800 LT and lasted for about 15 h. It had a peak wind period from 1130 to 1400 LT, with wind gusts consistently exceeding  $40 \text{ m s}^{-1}$  (90 mph). Wind gusts did not decrease in the vicinity of the fire until after 0100 LT 31 December 2021, when they dropped to under  $20 \text{ m s}^{-1}$  (45 mph).

### a. Observations

In this section, we document the development and evolution of the windstorm using several observational sites key to the location of the fire, as well as a collection of observations that cover the larger area from southern Wyoming to the Front Range of Colorado (terrain elevation shown in Fig. 4). We examined the larger collection of surface observations using the NOAA NWS Weather and Hazards Viewer (<https://www.wrh.noaa.gov/map/>). The observations available include standard METAR sites as well as a variety of other observations that, together, provide relatively good coverage of the larger area noted above. Despite some gaps, the observations provide an overview of how the strong winds evolved on 30 December 2021. A time series of observed wind-gust maps beginning at 1500 UTC 30 December through 0000 UTC 31 December is shown in Fig. 5.

At 1400 UTC (0700 LT), observed wind gusts  $> 35 \text{ m s}^{-1}$  (Fig. 5) were only evident in Larimer County at a single site but became evident southward in succeeding hours through Boulder County and into northern Jefferson County, maximizing at 1900 UTC. At 1500 UTC (0800 LT), the strongest winds were located in the mountains mainly east of the Continental Divide and just beginning to reach the lower foothills. As will be shown in section 3, the 400-hPa jet stream position and transverse wind speed gradient, also moving southward, determined the onset of the strongest winds in southern Boulder County and northern Jefferson County. Wind gusts subsided slightly by 0100 UTC but still exceeded  $35 \text{ m s}^{-1}$  at a few locations.

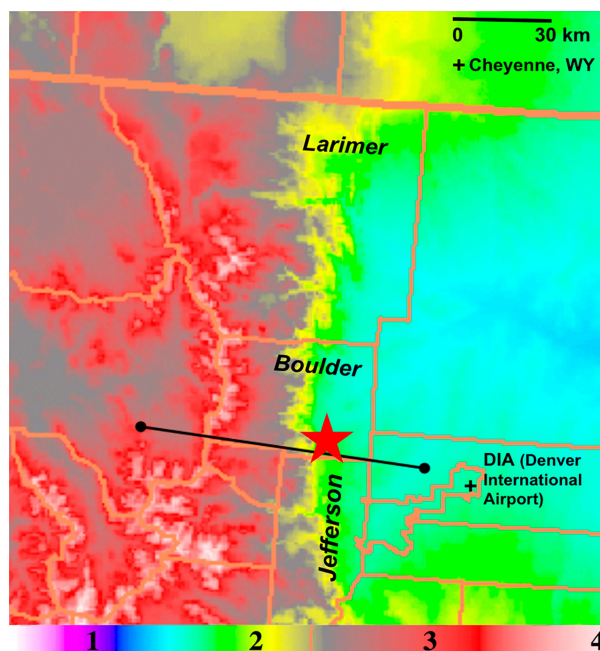


FIG. 4. Terrain elevation (km; color scale) for the Front Range area of Colorado and southern Wyoming. Boulder, Jefferson, and Larimer Counties in Colorado are also labeled. The horizontal line through southern Boulder County is the location for vertical cross sections presented later in Figs. 11 and 18. The Marshall Fire ignition location area (also in Fig. 6) is shown by the red star.

Wind-gust and wind-direction time series over a 24-h period for four key observation sites are shown (see Fig. 7). Figure 6 shows the location of these sites with respect to the outline of the fire burn area. The north–south dashed lines in Fig. 6 separate three general zones for the wind-gust speed behavior during the windstorm. As noted earlier in section 1a, the presence of a hydraulic jump within the mountain wave across the area of Fig. 6 resulted in much weaker winds just east of the eastern fire boundary that were often from the east to northeast in response to the horizontal rotor within the mountain wave. Wind gusts increased at each of these sites from 0900 to 1130 LT, peaking at the time of the fire ignition.

At the NCAR Mesa Laboratory (site 4 in Fig. 6), located approximately 2.5 km west of the BLD01 site and  $\sim 250 \text{ m}$  higher, an initial strong ramp-up in wind and gustiness also occurred near 1500 UTC (0800 LT). The behavior is similar to that from nearby BLD01 but different from the other more southern sites (NREL, 93–72), with a sharp decrease by 1600 UTC (0900 LT), followed by another more gradual increase of the winds toward 1800 UTC with peak gusts occurring in the afternoon from 2000 to 2230 UTC (1300–1430 LT). A contrast in wind direction is seen between the Boulder sites (NCAR, Southern Hills) with  $225^\circ$ – $245^\circ$  versus the NREL and CO93/CO72 stations further south with  $270^\circ$  shown (Figs. 7b and 8b). The Boulder-site wind directions from the southwest were unusual in that the typical surface wind direction during downslope windstorms is from west to west-northwest ( $270^\circ$ – $315^\circ$ ).



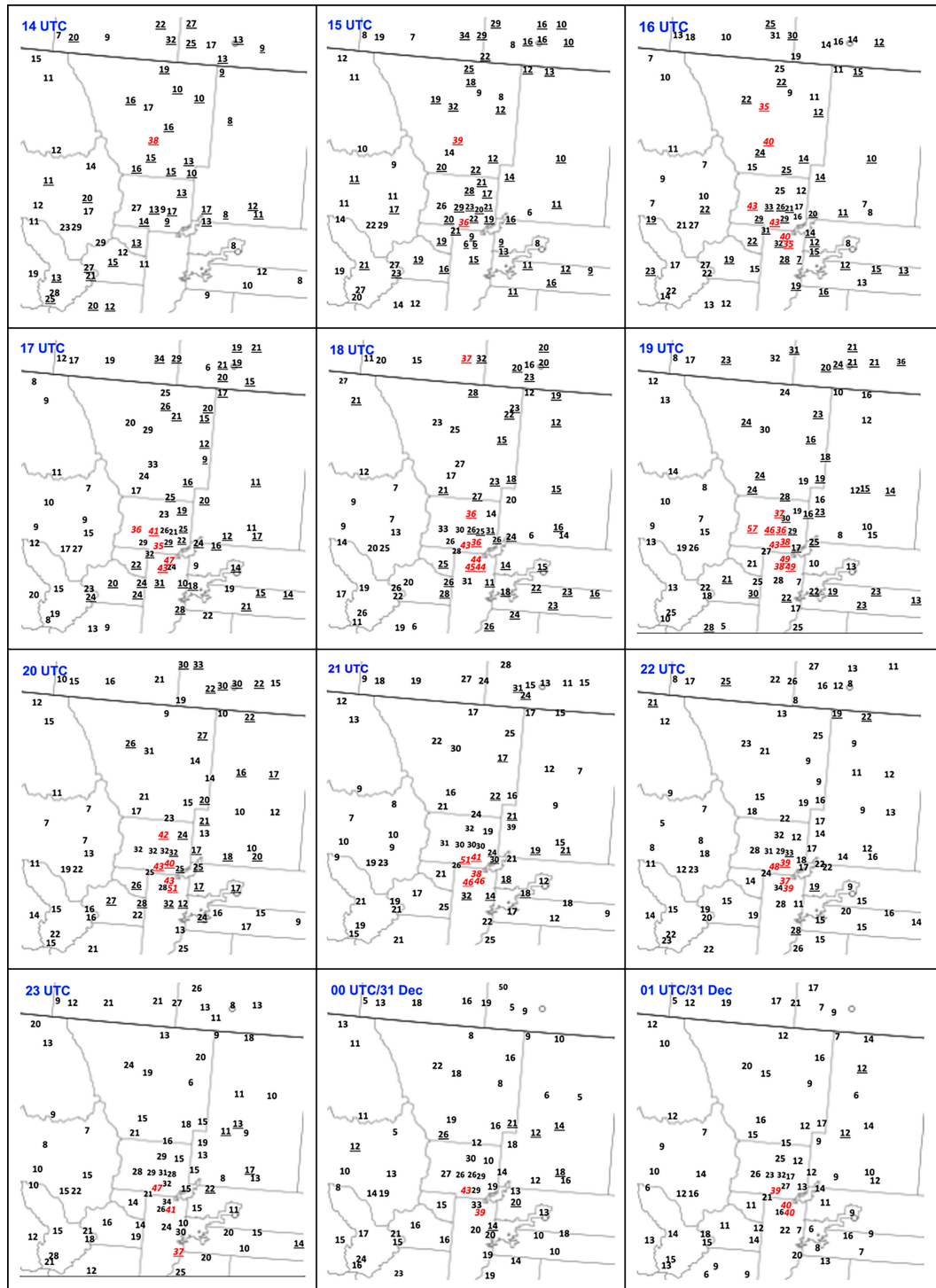


FIG. 5. Hourly plots of observed 10-m wind gusts ( $\text{m s}^{-1}$ ) from 1400 UTC 30 Dec 2021 to 0100 UTC 31 Dec 2021, as described in text. Red indicates wind gusts greater than  $35 \text{ m s}^{-1}$ . Underlined numbers represent a new maximum wind gust during the hour ending at the given time and also a new daily maximum wind gust (since 0000 LT, or 0700 UTC 31 Dec 2021).

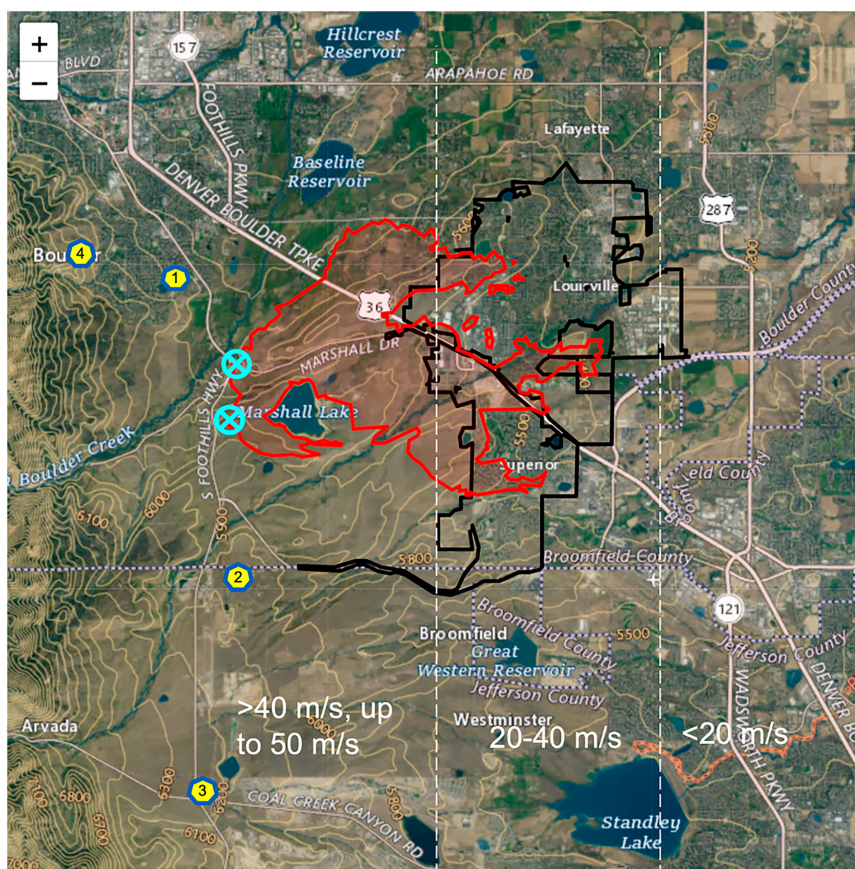


FIG. 6. Locations (yellow) of four stations in southern Boulder County and northern Jefferson County for which observed 10-m wind gust time series are shown in Figs. 7 and 8. 1) BLD01—Southern Hills Middle School in south Boulder. 2) NREL—National Wind Technology Center (NWTCT). 3) Intersection of Colorado state highways 93 and 72. 4) NCAR Mesa Laboratory. Also shown are the location of the Marshall Fire burn area (red) and the boundaries of the towns of Louisville and Superior (black outlines). Locations of ignition are shown (in cyan) south of Boulder as reported by the Boulder County Sheriff's Office (2023). Approximate zones for maximum wind gusts during 30 Dec 2021 are shown in white. (Base Google map from <https://www.denverpost.com/2021/12/31/marshall-fire-map-perimeter-boulder-county-wildfire/> including terrain elevation in ft.)

Returning to the reported wind gusts across the larger area in Fig. 5, the rapid increase in the winds shown in the time series is also seen on a broader scale, particularly across Boulder and Jefferson Counties between 1700 and 1900 UTC, with many new event-maximum hourly gusts occurring and spreading out from the Front Range onto the nearby plains. The  $57 \text{ m s}^{-1}$  gust shown at 1900 UTC in Fig. 5 (strongest gust observed in this study) is from a site located on Niwot Ridge west of Boulder at 3050 m MSL, approximately 8 km east of the Continental Divide. After 2000 UTC, however, we see a change from new event-maximum hourly gusts to gusts of lower magnitude. This trend continues after 2100 UTC with many gusts gradually decreasing, except for some modest new maximum hourly gusts farther east on the plains.

Unfortunately, even though the peak winds did decrease somewhat during the afternoon, as shown in the time series, they remained substantial with frequent gusts exceeding  $35 \text{ m s}^{-1}$ .

The general behavior of the windstorm was for the peak gustiness to gradually retreat toward the foothills and immediate areas near the foothills after 0500–0600 UTC (2200–2300 LT), providing relief for firefighters. Still, the real break did not arrive until a strong cold front with northeast winds and much colder temperatures passed the fire area around 0100 LT 31 December, followed by 18–25 cm of snow that began by the next afternoon.

One interesting aspect of this event was the strong, quick surface pressure drops over only a few minutes associated with the onset of the strong winds. Figure 8 shows time series of several available surface weather stations with barometer readings during the day on 30 December 2021; fixed pressure offsets are added to each station to allow for the time series to appear from north to south going from top to bottom in Fig. 8. A dramatic, sustained drop in surface pressure (3–6 hPa) moved southward along the Front Range during the 1400–1500 UTC 30 December period. However, not all surface stations observed this drop:

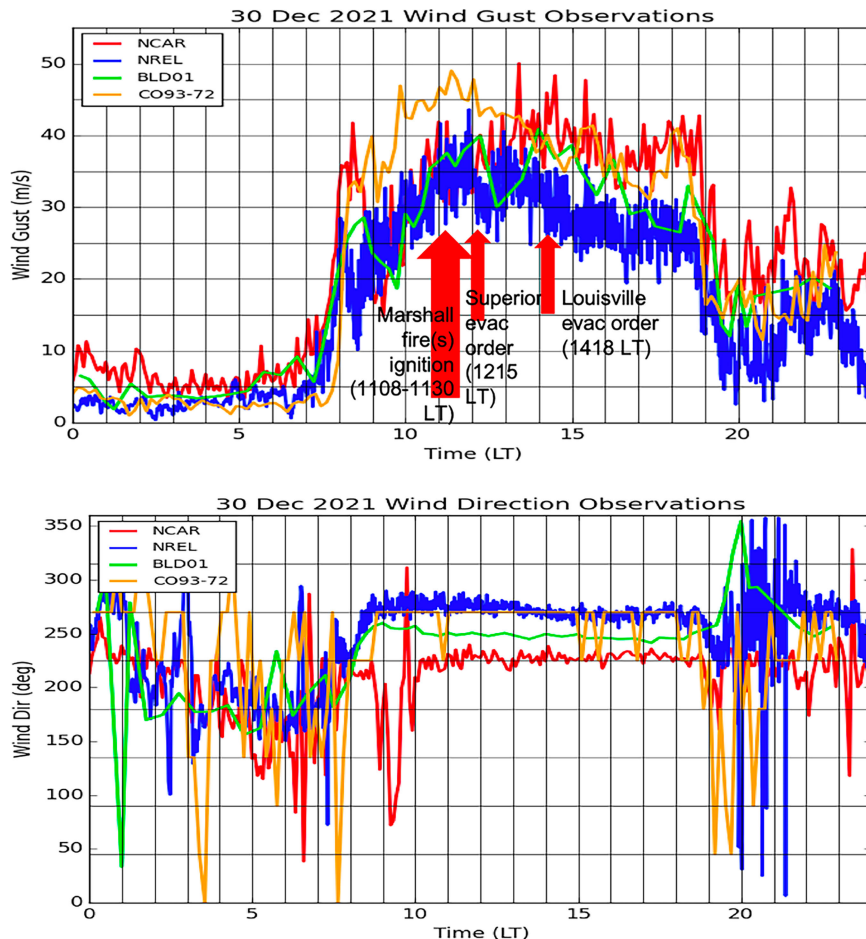


FIG. 7. Observed (top) wind-gust speed and (bottom) wind direction from four locations (NCAR Mesa Laboratory (red), Southern Hills Middle School in south Boulder (BLD01, green), NREL/NWTC (blue), and CO93/CO72 intersection (orange) shown in Fig. 6 from 0000 to 2300 LT (0700–0600 UTC) 30 Dec 2021. Key events for the Marshall Fire ignition and evacuations are also shown.

sites in Cheyenne, Wyoming (green trace), and at Christman Field in western Fort Collins, Colorado (black trace), did not exhibit a pressure drop. Sites that did not observe a pressure drop also did not experience high winds (not shown). The southward movement of the pressure drop appears to be associated with the southward migration of the poleward edge of the jet streak (see section 3), suggesting the features may be linked.

#### b. Wind-gust diagnostic analyses

We also examine the near-surface wind-gust evolution using proxy analyses of wind-gust potential (WGP; Benjamin et al. 2021). We approximate analyses while ensuring physical consistency from vertical mixing by using very short (1-h) forecasts from the 3-km HRRR model (Dowell et al. 2022; James et al. 2022), using a diagnosed WGP. This diagnostic provides a rough spatial estimate of wind-gust potential (Fig. 9) through a weighted combination of wind speeds in the planetary boundary layer (PBL) with the PBL depth diagnosed from the model vertical profile of virtual potential temperature  $\theta_v$ . It is designed to

estimate *potential* wind gusts and is higher than the mean observed wind gusts at a particular time. Fovell et al. (2022) showed that the HRRR WGP diagnostic (diagnosed from instantaneous fields) agrees well with observations for this case, while Fovell and Gallagher (2022) evaluated a different gust diagnostic also based on HRRR. As discussed in Benjamin et al. (2021), other wind fields are available to consider for wind-gust prediction including hourly maximum 10-m wind and instantaneous 80-m wind, but WGP has been most widely and effectively used to maximize the probability of detection for strong wind gusts (e.g., Fovell and Gallagher 2022; Fovell et al. 2022).

The HRRR 1-h WGP forecast valid at 1300 UTC 30 December (top left panel in Fig. 10) showed a 20–30  $\text{m s}^{-1}$  area from near the Continental Divide down to  $\sim 2000\text{-m}$  elevation. Areas with stronger WGP up to 30–35  $\text{m s}^{-1}$  and then exceeding 40  $\text{m s}^{-1}$  became evident first in Larimer County in Colorado closer to the Wyoming border from 1400 to 1500 UTC, then building southward through Boulder County into Jefferson County by 1600 UTC. For this field, the strongest WGP ( $>40 \text{ m s}^{-1}$ ) was



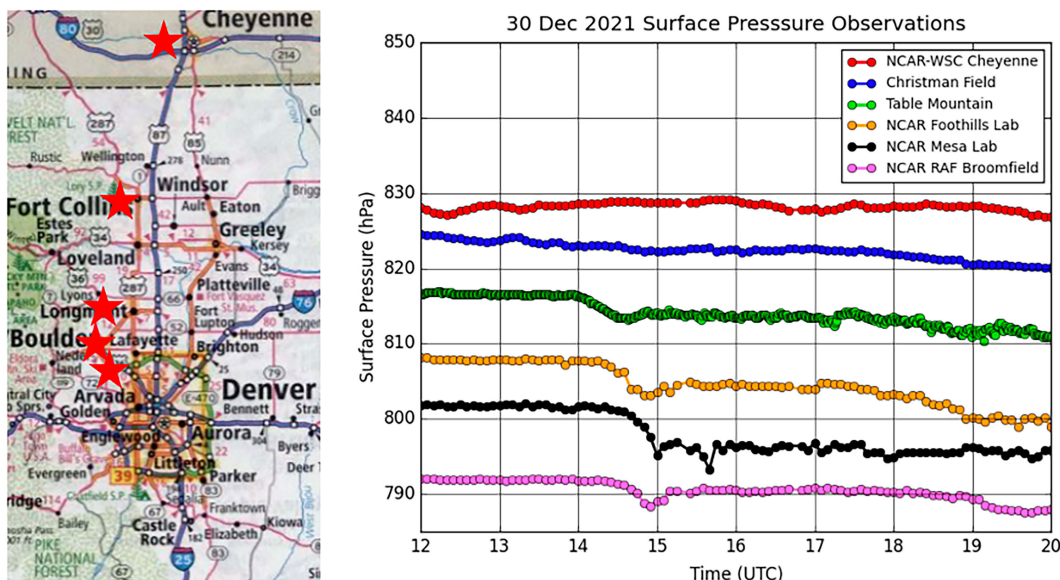


FIG. 8. Surface pressure observations from six surface sites from Cheyenne, WY, southward through Boulder (Table Mountain north of Boulder, then NCAR FL and ML sites) to Broomfield, CO, during 30 Dec 2021. Arbitrary pressure offsets are added to the stations to allow them to be displayed from north to south going from top to bottom.

evident for 1900–2000 UTC, then tapering off slightly to  $30\text{--}35\text{ m s}^{-1}$  by 2300–0000 UTC. We consider this depiction in Fig. 10 as representing the larger-scale evolution of the wind profile in the diagnosed boundary layer including the peak winds from 1600 to 2100 UTC, but not necessarily matching the detailed wind-gust observations provided in Fig. 5.

### c. Fire ignition

The months in 2021 leading up to the Marshall Fire were exceptionally warm and dry in the Colorado Front Range region, with near-record mean temperatures and near-record low precipitation over the last half of the year. This warm and dry 6-month period without virtually any snow (National Weather Service 2021) followed an unusually wet spring and early summer in Boulder, leading to rapid curing of heavy fine fuels including tall

grasses. As of 28 December 2021, the U.S. Drought Monitor showed extreme drought conditions (D3) in Boulder County. These conditions began to lead to small wildfires in the autumn. Another measure of potential fire growth and spread based on fuels is the energy release component (ERC), which represents the amount of heat per area released during flaming (Jolly et al. 2019). The morning before the Marshall Fire ignited, ERC percentiles were at the 80th–90th percentile in the vicinity and >95th percentile in proximity to the south and east, pointing to the abnormally wet spring followed by a dry autumn and early winter. During the 30 December 2021 windstorm, several fires ignited in the Boulder vicinity; however, all but two were quickly extinguished. The Middle Fork Fire, west of Longmont, threatened homes and destroyed some structures but was contained relatively quickly, while the Marshall Fire south of Boulder rapidly grew beyond control.

An official Marshall Fire Investigative Summary and Review was issued by the Boulder County Sheriff's Office (2023) in June 2023. This report confirmed two ignition locations (Fig. 6), one near the intersection of CO93 and CO170 near the town of Marshall and one about 0.5 km south of Marshall. For all ignition sources considered in the report, “extraordinarily high” winds were the cause, either through providing fresh oxygen (to an extinguished 6-day-previous small burn) or through unmooring of powerlines. An ongoing coal seam fire was not found to be the most likely ignition source for the southern ignition but not ruled out. Extreme winds providing the oxygen source leading to coal seam autocombustion (Lu et al. 2017) were considered as a possible ignition source. As of 2018, 38 coal seam fires had been identified in Colorado including two near Marshall (Colorado Department of Natural Resources 2018, 14–17); many others have been identified globally (e.g., Kuenzer and Stracher 2012).

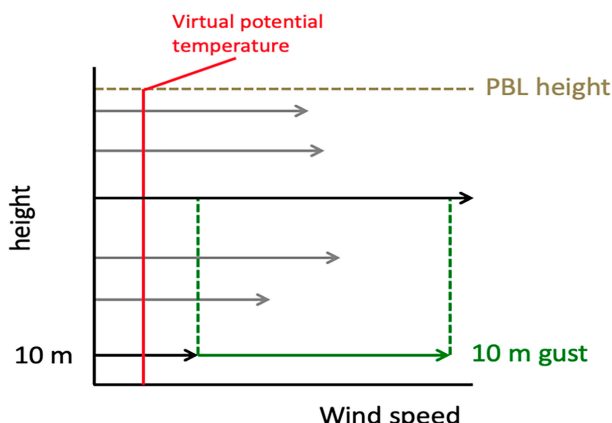


FIG. 9. Representation of WGP diagnostic applied to wind profiles using the diagnosed boundary layer height. Extracted from Benjamin et al. (2021, NOAA Tech. Memo).

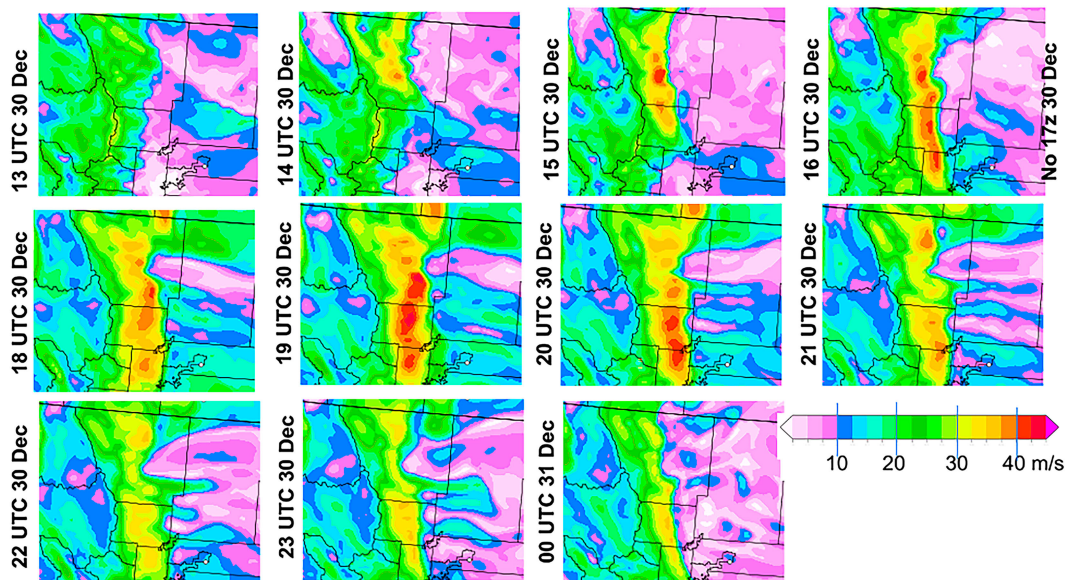


FIG. 10. Hourly gridded 10-m WGP ( $\text{m s}^{-1}$ ) (HRRR 1-h forecasts) valid at 1300 UTC 30 Dec 2021–0000 UTC 31 Dec 2021.

Firefighters arrived on the scene within minutes of the ignition(s), but wind gusts over  $50 \text{ m s}^{-1}$  made it impossible to get the flames under control, even when there was only a small area on fire (Colorado Division of Fire Prevention and Control 2022). The fire quickly spread to the east and burned across nearly 5 km of widely scattered homes and grasslands in less than an hour. By 1200 LT, it reached the urban interface in Superior, and from there, it spread quickly from house to house. The fire reached the densely populated part of Louisville after crossing U.S.-36 between 1230 and 1245 LT. One of the main reasons for rapid spread was ember transport (“spotting”) with the extreme winds (Colorado Division of Fire Prevention and Control 2022). Even a broad, six-lane freeway like U.S.-36 did little to slow the spread of the fire. For the remainder of the afternoon into the early evening, the fire burned homes and businesses. Next, we examine the three-dimensional wind flow that fueled the fire.

### 3. Evolution of the event from a three-dimensional wind-flow perspective

Downslope windstorms at the surface are driven by the three-dimensional wind flow and stability structure, as described in section 1a using descriptions from Durran (1986). Here, we examine observations and analyses to examine the 3D structure for the Colorado 30 December 2021 windstorm to complement the near-surface perspective just discussed in section 2.

#### a. Vertical cross sections—west–east through Marshall—from HRRR

Vertical cross sections (Fig. 11; surface to 300 hPa) along a west–east line cutting through southern Boulder County from HRRR analyses show the evolution of the wind and stability profile associated with the flow evolution at 400 hPa shown later in

Figs. 12 and 13. During the overnight period of 29–30 December, increasingly strong upper-level flow appears across the Continental Divide, with speeds exceeding  $60 \text{ m s}^{-1}$  (Figs. 11e). The upper-level flow shows signs of weakening at 1500 UTC (Fig. 11f), and a signal of strong descent (shooting flow) begins to appear east of the mountains (seen particularly for the 300–308-K isentropes). By 1700 UTC (Fig. 11g), the downslope windstorm is underway, with strong subsidence along the east slopes of the Front Range (296-K isentrope now located far closer to the surface), and  $40+ \text{ m s}^{-1}$  flow now nearing the surface extending down the foothills. This pattern persists at 2100 UTC, with flow weakening by 0000 UTC at least in these cross sections through southern Boulder County.

Juliano et al. (2023) also modeled the 30 December 2021 windstorm with a 111-m resolution version of WRF-Fire initialized with HRRR data. They show a hydraulic jump at the east end of the high-wind region. In the 3-km operational HRRR forecasts, a similar but more coarsely defined convergence zone and hydraulic jump is evident at 1700 UTC (Fig. 11g) with wind exceeding  $35 \text{ m s}^{-1}$  extending to eastern Boulder County, approximately coinciding with its definition of the zone of strong upward motion.

#### b. 400-hPa wind analyses

As described by Fovell et al. (2022), the setup for the 30 December 2021 Front Range downslope windstorm was produced by a favorable wind and stability profile and a region of light winds aloft evident in their figures for winds near 400 hPa.

Figure 12 shows HRRR wind analyses at 400 hPa over the contiguous United States (CONUS) every 3 h in the 24 h leading up to the windstorm onset. As shown by Fovell et al. (2022), the HRRR captured the evolution of the upper-level flow, particularly at short forecast durations. HRRR analyses are considered a realistic estimate of the state of the atmosphere.

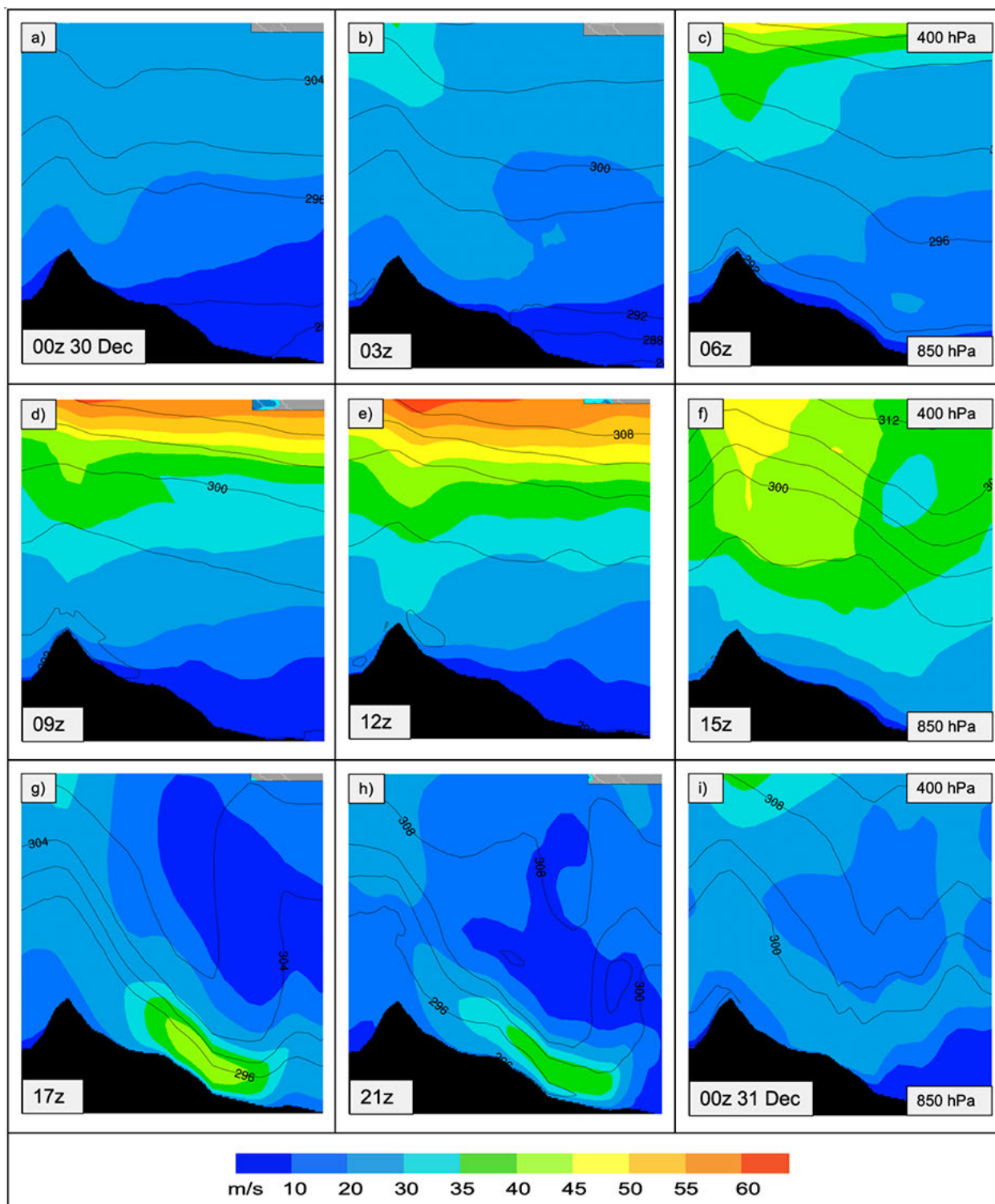


FIG. 11. West-east cross sections of HRRR analysis wind speed ( $\text{m s}^{-1}$ , color) and isentropes from 850 up to 400 hPa through southern Boulder County (location in Fig. 4), at (a) 0000, (b) 0300, (c) 0600, (d) 0900, (e) 1200, (f) 1500, (g) 1700, and (h) 2100 UTC 30 Dec and (i) 0000 UTC 31 Dec 2021.



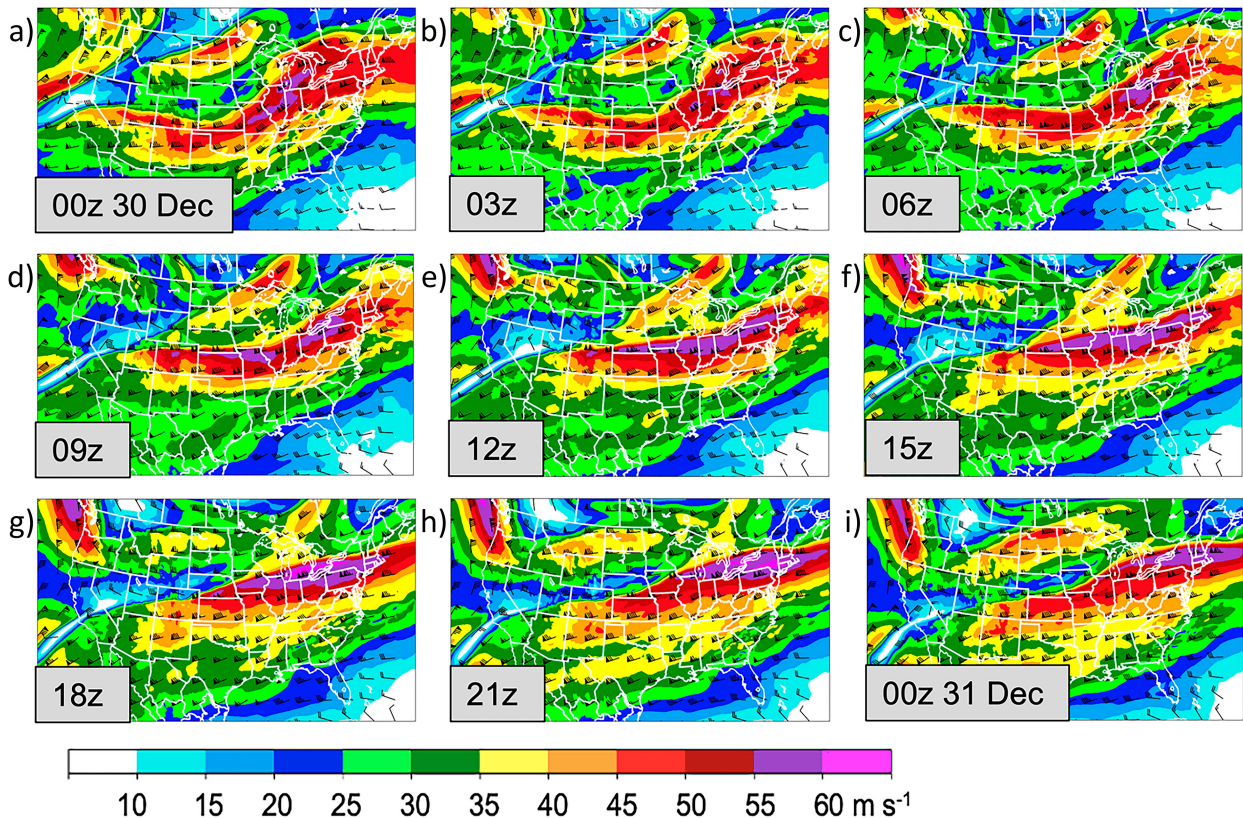


FIG. 12. The 400-hPa winds over CONUS from HRRR analyses ( $\text{m s}^{-1}$ ), valid at (a) 0000, (b) 0300, (c) 0600, (d) 0900, (e) 1200, (f) 1500, (g) 1800, and (h) 2100 UTC 30 Dec 2021 and (i) 0000 UTC 31 Dec 2021.

The complexity of the tropospheric pattern over the CONUS during the 30 December 2021 event is evident in the 3-hourly sequence of 400-hPa wind analyses in Fig. 12. During the 24-h period in Fig. 12, a  $55+ \text{ m s}^{-1}$  west-to-southwesterly extended jet stream at 400 hPa is situated across the Midwest from Nevada eastward to New England, initially exhibiting cyclonic curvature from the southern High Plains to the central Great Lakes but evolving into a more linear jet streak after 1200 UTC 30 December. During this overnight period, a smaller west-to-southwesterly jet streak is seen farther north, from the Dakotas into western Ontario, which lifts farther northeastward, out of the HRRR domain, later in the day. In the meantime, a strong northerly jet begins to dig southward along the Pacific Northwest coast. An important feature for the Colorado downslope windstorm is the positively tilted trough axis extending initially from Oregon to central Montana and its effect on the southward shifting of the larger-scale west-to-southwesterly jet across the United States southward over Colorado with the onset of the windstorm.

Figure 13 shows more detail of the 400-hPa flow in the vicinity of Colorado. The latitudinal movement of the large-scale jet including over Colorado can be seen during this period, with the jet lifting northward during 0000–0900 UTC and then sinking southward later in the day. At the same time, the westerly flow at the north edge of the jet dramatically decreases between 1200 and 1500 UTC 30 December. The vertical profile of the analyzed

HRRR wind speed at 1600 UTC is provided by Fovell et al. (2022, their Fig. 11). The net result of this evolution is the onset of an extreme north–south gradient in zonal wind ( $>40 \text{ m s}^{-1}$  in  $\sim 50 \text{ km}$ ) signaling a local shift to the left rear jet quadrant (Uccellini and Johnson 1979) in Boulder County (Fig. 13f), implying intense descent in this region. The gradient persists at least until 2100 UTC based on these HRRR analyses. The southward movement of the 400-hPa jet creates a favorable environment for the mountain wave, whose signature is superimposed on the larger-scale 400-hPa flow (e.g., Fig. 13f). Given the small horizontal scale of the strong gradient in 400-hPa wind speed, it is not surprising that even CAMs (convection-allowing models) like the HRRR could have struggled to predict the exact location at the exact onset time with advanced lead time.

#### c. Vertical profiles from raobs, commercial aircraft, and analyses

Examining the sequence of raob soundings (Fig. 14) from Grand Junction (GJT) and Denver (DNR), a midlevel inversion first appears at 0000 UTC 30 December in the DNR sounding, located near 520–550 hPa (Fig. 14b). An inversion is seen with similar magnitude at GJT, but situated near 600 hPa (Fig. 14c). Dramatically increasing midtropospheric wind speeds are seen from 1200 UTC 29 December to 1200 UTC 30 December, with  $50+ \text{ m s}^{-1}$  flow seen at DNR at 1200 UTC 30 December

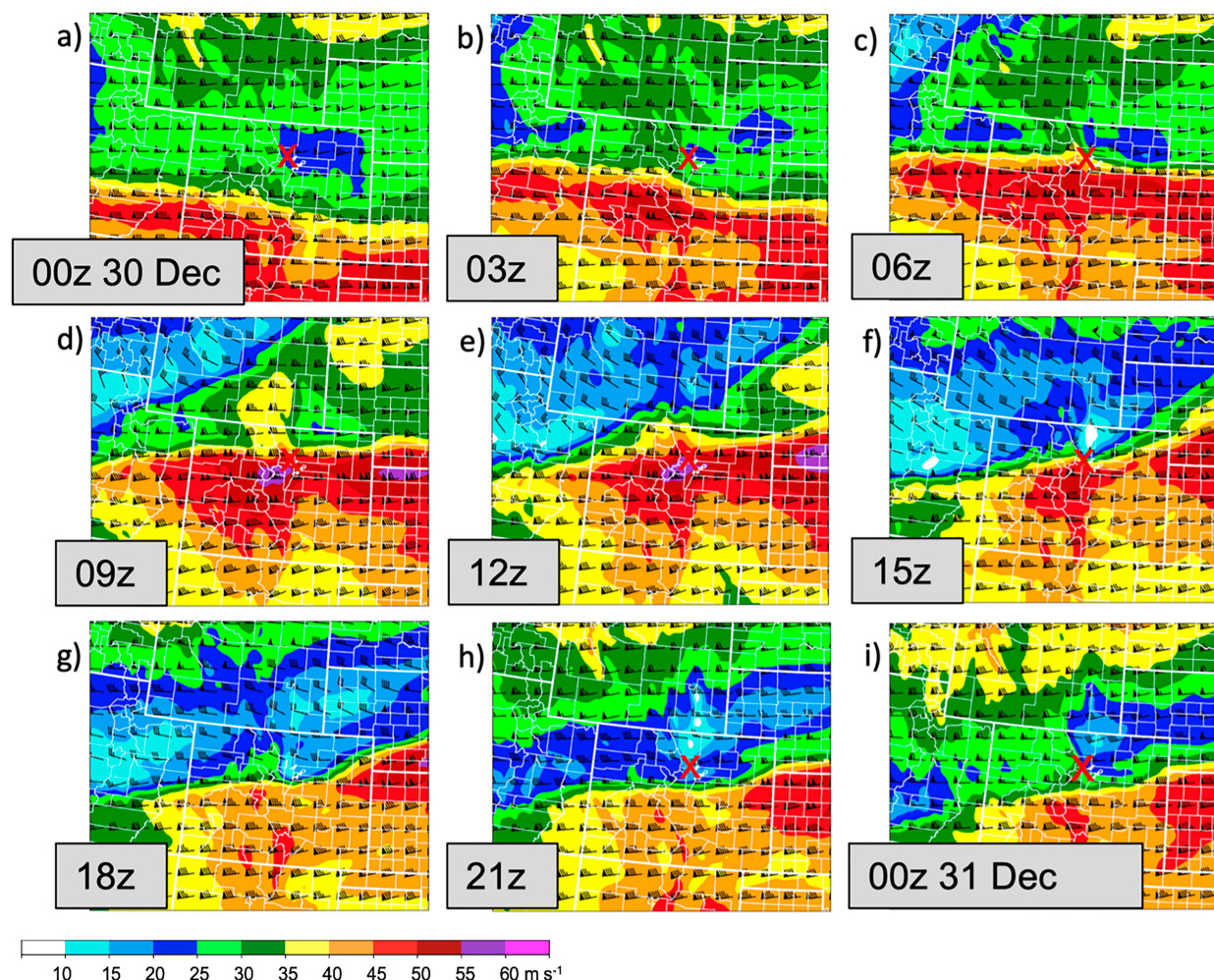


FIG. 13. As in Fig. 12, but showing only the Colorado–Wyoming vicinity. Valid at (a) 0000, (b) 0300, (c) 0600, (d) 0900, (e) 1200, (f) 1500, (g) 1800, and (h) 2100 UTC 30 Dec 2021 and (i) 0000 UTC 31 Dec 2021.

between 250 and 400 hPa (Fig. 14d). By 1200 UTC 30 December, a few hours before the beginning of the windstorm, the DNR sounding sampled an inversion near 450–470 hPa, while the GJT sounding indicated a deeper isothermal layer from 440 to 500 hPa. By 0000 UTC 31 December, as the windstorm was ending, the DNR sounding revealed that this deep isothermal layer had intensified into a  $\sim 4$ -K inversion, and its base had subsided to 600 hPa and now with much drier conditions, both indicating strong descent over the preceding 12 h.

Aircraft soundings (Fig. 15) provide a more complete picture of the evolution of the relevant flow features after 1200 UTC 30 December. Denver International Airport, as a major worldwide airport hub, hosts numerous ascent and descent observations each day, some of which contain moisture observations. It is important to note that aircraft ascents are made at a much steeper angle than descents (e.g., James et al. 2020), thus sampling a higher altitude region near the airfield than descents from the same direction. Figures 15a and 15b show ascent and descent soundings taken near the same time, although at slightly different directions (with the aircraft descent sampling farther north than the ascent).

The thermodynamic profiles of the first two aircraft soundings look similar (Figs. 15a,b), with relatively well-mixed conditions below 600 hPa and stable stratification above this. The wind profiles both show a region of light winds near 400–500 hPa, with stronger westerly flow above and below this level; the ascent sounding, farther south, samples stronger flow in both the upper and lower levels. Both soundings place the wind minimum at  $\sim 460$  hPa, with the southern ascent sounding indicating a minimum of  $10 \text{ m s}^{-1}$ . An ascent sounding taken through a similar region about an hour later (Fig. 15c) reveals that strong subsidence has occurred in the 600–450-hPa layer, with an inversion at the base (580–550 hPa). This sounding also indicates flow  $< 8 \text{ m s}^{-1}$  ( $\sim 15$  kt) near 450 hPa. An aircraft descent sounding taken an hour later indicates continued subsidence above 600 hPa (Fig. 15d). Taken together, these aircraft observations suggest that intense subsidence was occurring during the day coincident with the formation of the mountain wave, with a region of light winds separating vertically the upper-level jet from a strong downslope windstorm below 500 hPa, consistent with the classic downslope vertical structure evident at 1700 UTC in Fig. 11g.



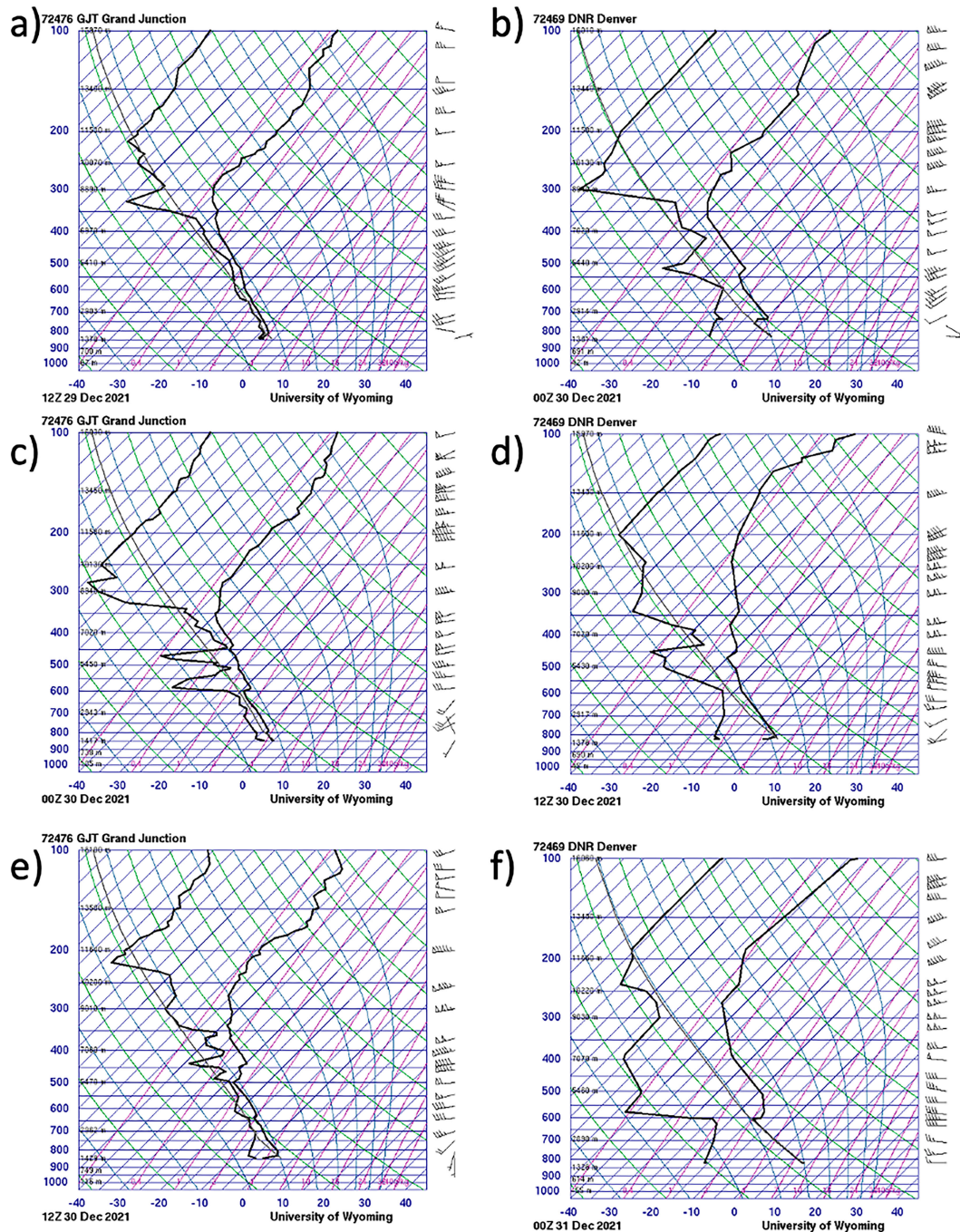


FIG. 14. Rawinsonde observations from (left) Grand Junction and (right) Denver at (a) 1200 UTC 29 Dec; (b),(c) 0000 UTC 30 Dec; (d),(e) 1200 UTC 30 Dec; and (f) 0000 UTC 31 Dec 2021.

There was a major wind shift between 1500 and 1600 UTC evident when comparing Figs. 16a and 16b. A significant stable layer appears between 500 and 600 hPa, and wind speed around 420 hPa decreases from almost  $25 \text{ m s}^{-1}$  to under  $10 \text{ m s}^{-1}$ , consistent with the southward shifting of the large-scale jet evident in Figs. 12 and 13 between 1500 and 1800 UTC. This southward shift was evident in the aircraft soundings shown in Fig. 15 and

coincident with the onset of the initial windstorm between 1500 and 1600 UTC as shown in Figs. 4 and 5.

#### d. Nonclassical jet/wave pattern for this event

There were several aspects in which this event did not match the classical synoptic-scale upper-air pattern described in section 1a and in Mercer et al. (2008). As described in that paper,



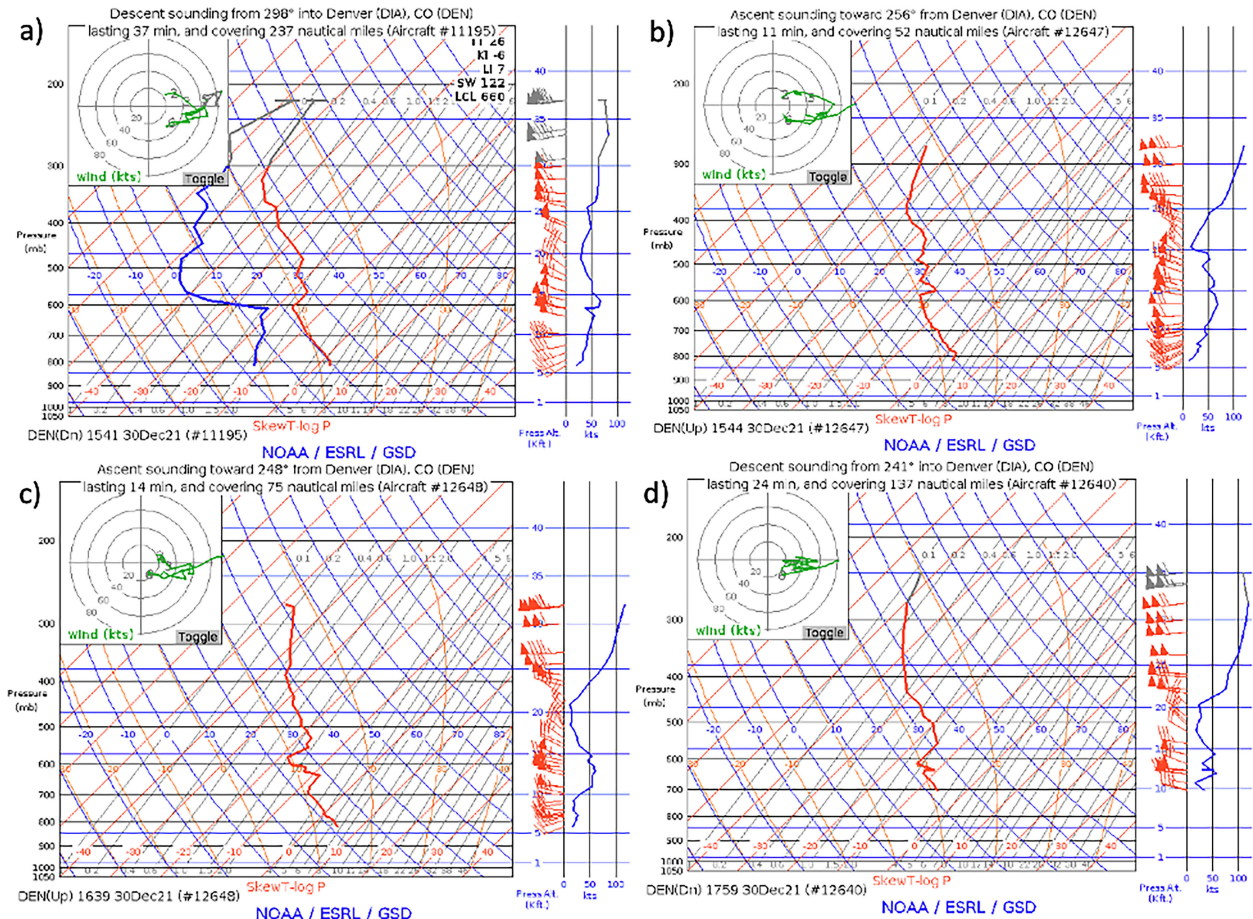


FIG. 15. Commercial aircraft soundings from ascents from or descents into Denver on 30 Dec 2021. Shown are (a) descent sounding from 298° direction (WNW) at 1541 UTC, (b) ascent sounding toward 256° (WSW) at 1544 UTC, (c) ascent sounding toward 248° (WSW) at 1639 UTC, and (d) descent sounding from 241° (WSW) at 1759 UTC. Wind barbs are in knots ( $1 \text{ kt} \approx 0.51 \text{ m s}^{-1}$ ).

there are two general synoptic patterns that are associated with severe downslope windstorms in Boulder County. These can loosely be described as “warm advection” and “cold advection,” with each being associated with a progressive short-wave trough at mid- and upper-tropospheric levels. Prominently, the 400-hPa wind structure for this event (Figs. 12 and 13) showed a continent-crossing jet with west-southwest flow from California to Maine without a well-defined embedded short-wave trough aloft. This differs from the classic pattern for midwinter severe windstorms of a progressive short-wave trough embedded in broader-scale west-northwest flow shown in Fig. 3 and Lilly (1978, their Fig. 4). Further, strong surface cyclogenesis on the High Plains east or northeast of Boulder, typical of cold-advection windstorms, was also lacking. In addition, the surface wind direction in Boulder (NCAR, Southern Hills) was also from the southwest (e.g., Fig. 7b) and not from the usual due-west direction. We do not have an explanation for this local anomaly. Finally, the 2-m temperature on the plains held roughly steady throughout the event at  $5^{\circ}$ – $7^{\circ}\text{C}$ , neither with a sudden surface temperature increase with onset as with a typical warm-advection event, nor with strong surface cold advection behind a Pacific cold front moving across the mountains from the west as with a cold-advection event. The spread of high

winds onto the plains eastward through Louisville and Superior (see Fig. 6) also differs from the classic warm-advection event with persistent high winds typically limited to within 5 km of the foothills and also from the classic cold-advection event with very strong winds spreading across much of northeastern CO.

#### 4. Model prediction for the windstorm event

We now examine forecast guidance for the 30 December 2021 windstorm event using the same surface and upper-air and vertical cross-section fields examined for analyses in sections 2 and 3. Forecasts are shown from the NOAA GFS (Global Forecast System) model first but primarily from the HRRR model. HRRR forecasts are run hourly out to 18 h, and every 6 h, out to 48 h (Dowell et al. 2022, their Table 4). This forecast duration configuration, driven by operational computer resources, provided a limit of only  $\sim 15$  h before a potential weather event for examining hourly run-to-run consistency from the HRRR.

##### a. Outlooks from earlier in the week

Upper-level wind forecasts from at least 2 days before the Boulder County windstorms suggested the possibility for high

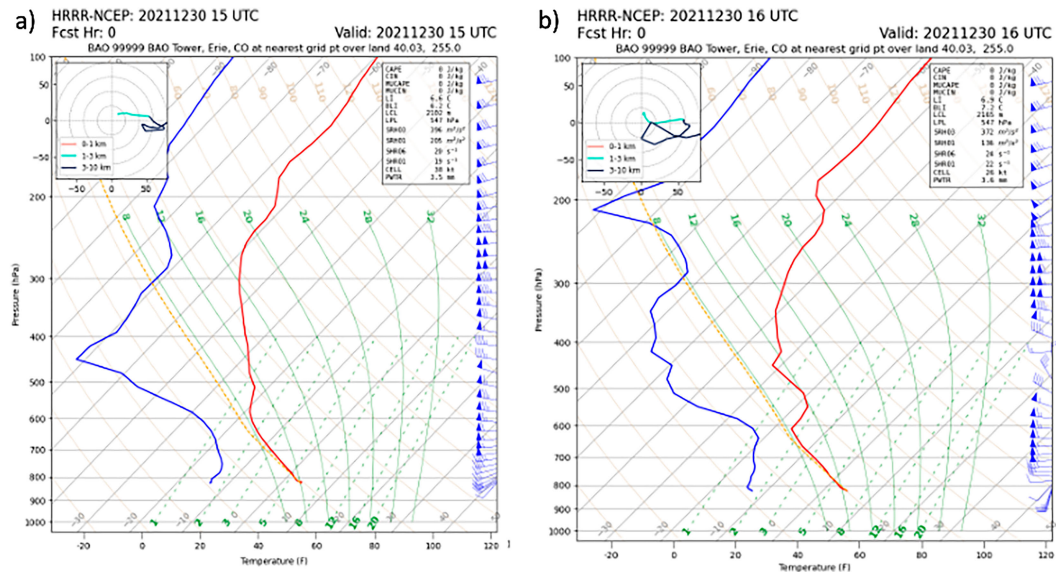


FIG. 16. HRRR-NCEP soundings (analyses) at the BAO tower site near Erie, CO, at (a) 1500 and (b) 1600 UTC 30 Dec 2021. Wind barbs are shown in knots.

winds near the surface at least for higher-elevation regions in Colorado. Based on the NOAA GFS forecast from 2 days before the event (initialized 1200 UTC 28 December 2021), NWS forecasters issued a High Wind Watch for 30 December 2021, as is discussed further later in section 5. The GFS 54-h forecast (Fig. 17) predicted 700-hPa winds of  $35 \text{ m s}^{-1}$  in the immediate lee of the northern Front Range valid at 1800 UTC 31 December (Fig. 17b), and a 400-hPa wind forecast (Fig. 17a) that compared well with the HRRR analysis at the same time (Fig. 14g).

#### b. Forecasts of vertical cross sections from the HRRR model

Previously in section 3, a set of west–east vertical cross sections from analyses are presented in Fig. 11 to examine the cross-section structure of the downslope windstorm (e.g., Fig. 2), complementing the horizontal WGP analyses in Fig. 10.

Here, we now examine HRRR forecasts in the same framework. Vertical cross sections (again from 400 to 850 hPa) of forecasts were examined from the HRRR model starting at 1200 UTC 29 December (Fig. 18) for a potential onset of downslope winds (defined here as wind speed  $> 30 \text{ m s}^{-1}$  within 200 m of the surface). The 1200 UTC 29 December HRRR forecast indeed showed a classical downslope wind structure but not until 2300 UTC 30 December, about 8 h later than observed. With the assimilation of newer observations, subsequent HRRR forecasts identified the same downslope structure but with an earlier onset, predicted at 2100 UTC (1800 UTC 29 December HRRR forecast) and at 1800 UTC (0000 UTC 30 December forecast). From that time (0000 UTC) onward, hourly HRRR forecasts showed a similar prediction with onset forecast slightly earlier, at about 1700 UTC (0600 UTC initialization). This examination of the 3D cross-section wind structure in Fig. 18 shows a consistency in the prediction of downslope winds over the plains from the sequence of HRRR forecasts but

with an earlier onset as newer observations were assimilated, apparently correcting small but significant large-scale errors in jet structure. With the HRRR forecast duration configuration (limited to 18 h for hourly forecasts), hourly consistency for forecasts valid at 1800 UTC 30 December was possible only starting with the 0000 UTC 30 December run.

#### c. 10-m wind-gust potential—HRRR forecasts

As shown for analyses in section 2b, we now examine predictions of wind-gust potential (WGP) from HRRR for the 30 December 2021 event. In Fig. 19, selected forecast valid times (1500–2100 UTC) during the daytime on 30 December are shown from four HRRR earlier runs (similar to those shown for cross sections in Fig. 18). It is clear from the different runs that there was an increasing threat of a windstorm along the Front Range with time, with a focus centered on eastern Boulder County. All of these forecasts show a high-WGP signature moving from north to south, consistent with the north–south jet shift. Consistent with Fig. 18, the 1200 UTC 29 December HRRR run (Fig. 19, top row) was slow to develop strong winds (event onset at 2300 UTC, not shown but shown in vertical cross section in Fig. 18) and at 2000 UTC for the 1800 UTC 29 December run (Fig. 19, second row). A significant shift occurred with the 0000 UTC 30 December run, with a much better forecast of strong winds in Boulder County in morning hours (1800 UTC and before). The 0600 UTC 30 December run similarly predicted WGP in excess of  $40 \text{ m s}^{-1}$ , as had other hourly HRRR forecasts in between (not shown). This run-to-run consistency once within 18 h of the possible event was important in interpretation by forecasters as described later in section 5.

Figure 20 shows the complete set of HRRR WGP forecasts valid at 1800 UTC 30 December, or just before the Marshall Fire began. The 48-h HRRR forecasts are initialized every 6 h, but the 1800 UTC 28 December run (upper left in Fig. 20)

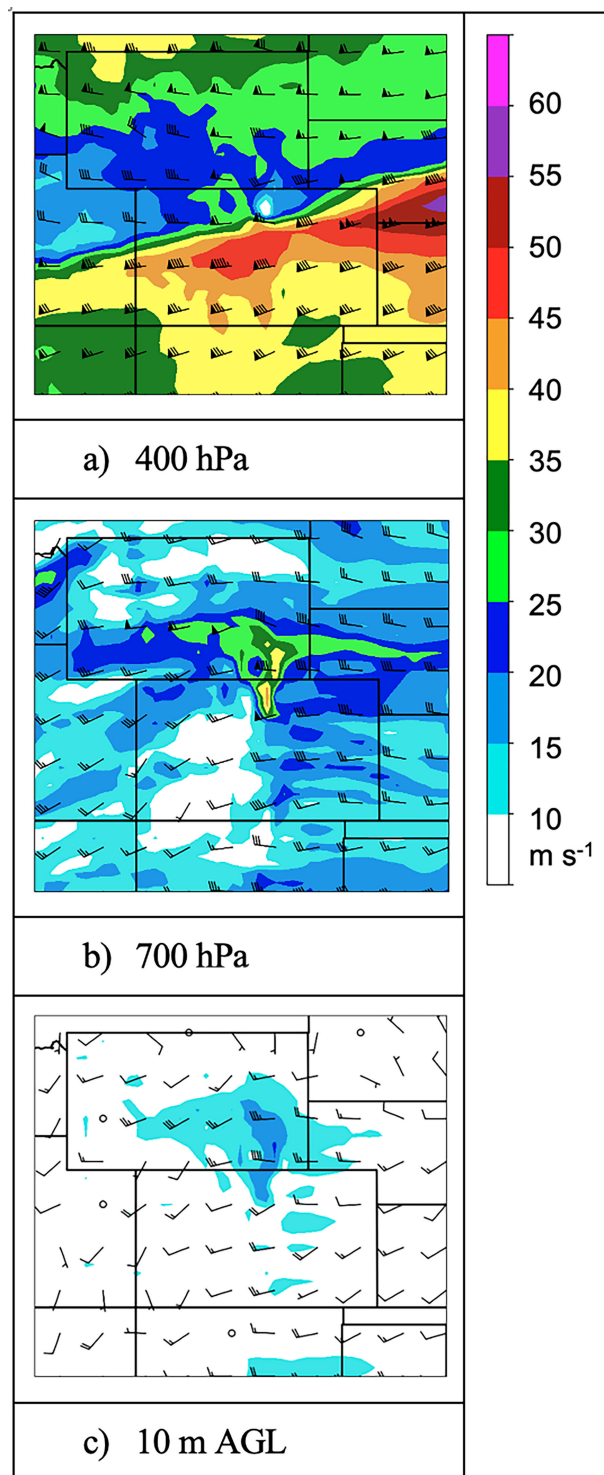


FIG. 17. The 54-h GFS wind forecasts ( $\text{m s}^{-1}$ ) valid at 1800 UTC 30 Dec 2021 from run initialized at 1200 UTC Tuesday 28 Dec 2021 for (a) 400 hPa, (b) 700 hPa, and (c) 10 m AGL.

showed no near-foothills windstorm at 1800 UTC 30 December (and delayed to 2100 UTC per Fig. 18). The 0000 UTC 29 December HRRR forecast did show a windstorm but not until 2300 UTC 30 December (bottom-left panel in Fig. 18). The main message from this set of forecasts is that beginning with the 0000 UTC 30 December run, there is a strong consistency in the forecast of a strong windstorm event with gusts exceeding  $40\text{--}45 \text{ m s}^{-1}$  by 1800 UTC 30 December, focused mainly either side of the eastern half of Boulder County and northern Jefferson County. These wind-gust values are not typically found in HRRR predictions of most wind events along the Front Range, so the high values, coupled with the run-to-run consistency of the forecasts, gave forecasters more confidence that a high-wind event east of the foothills would occur on 30 December.

#### d. 400-hPa winds—HRRR

Figure 21 shows the evolution from different HRRR forecasts matching the set of forecasts shown for 10-m WGP in Fig. 19. The southward movement of the westerly jet is evident even in the 1200 UTC 29 December run, but with the shift and sudden reduction in 400-hPa wind over Larimer and Boulder Counties not occurring until after 1800 UTC. The overall location of the 400-hPa jet valid during this 1500–2100 UTC 30 December period trended southward starting with each consecutive run and especially with the 0000 UTC 30 December run, in which the 400-hPa wind speed over central Boulder County decreased from almost  $50 \text{ m s}^{-1}$  at 1500 UTC down to under  $20 \text{ m s}^{-1}$  by 3 h later.

### 5. Operational products and services for the windstorm and Marshall Fire

For operational forecasters, prediction of downslope winds is a difficult process, especially along the Front Range of Colorado. NWP forecasts usually show some run-to-run variations for local details that are critical for public forecasts of downslope winds. Global numerical weather prediction can help forecasters identify ingredients days in advance, but rarely do the global models accurately predict the local magnitude, location, and timing of winds because of their coarse horizontal resolution. Forecasters at the NWS Forecast Office in Boulder understand global model limitations and focus on identifying the right ingredients favorable for downslope winds and then fine-tune the forecast and expected impacts once high-resolution model data are available. Earlier in the week before the Marshall Fire, global models were consistently showing unusually strong flow in the 400–700-hPa layer (GFS forecast in Fig. 17), and forecasters responded by issuing a High Wind Watch for the mountains and foothills of Jefferson, Boulder, and Larimer Counties above 6000 ft MSL on Tuesday 28 December, expecting high winds on Thursday 30 December. A timeline of the NWS bulletins for the 30 December 2021 event, including this High Wind Watch (meeting NWS criteria)<sup>1</sup> from 28 December, is provided in Fig. 22. As with most mountain wave-induced downslope

<sup>1</sup> High-Wind Warning criteria as of August 2023: <https://www.weather.gov/ctp/wwwCriteria>.



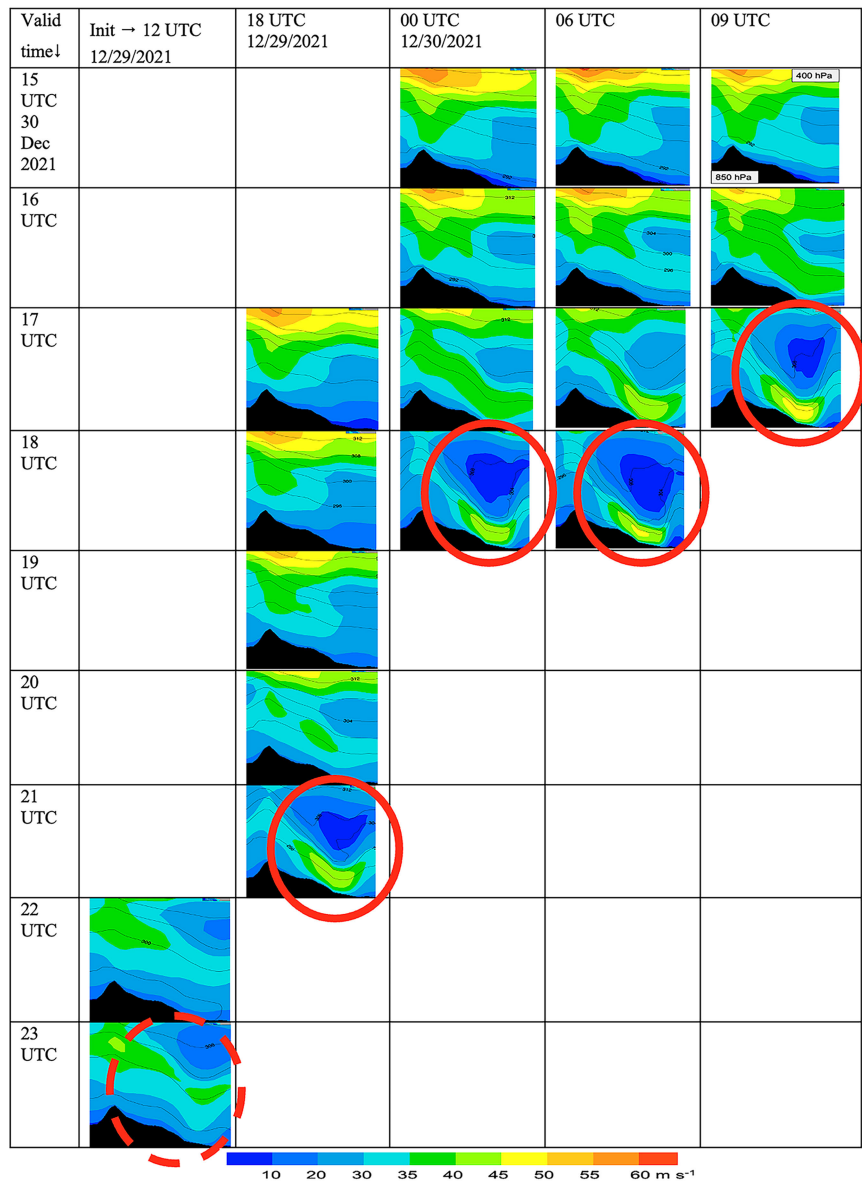


FIG. 18. West-east vertical cross sections of horizontal wind speed (through Marshall, CO, as in Fig. 11, location in Fig. 4) but now with matched valid times for HRRR forecasts from different initial times. The first forecasts from each HRRR run showing the classic downslope wind signature (Fig. 2 and section 1a) with sustained wind of at least  $30\text{ m s}^{-1}$  (shaded cyan) within 200 m of the surface are circled in red.

wind events, the hardest part of the forecast is whether the high winds would emerge east of the foothills, impacting the heavily populated corridor from Lyons (in northern Boulder County) to Boulder to Golden (in northern Jefferson County). At 48–72 h out, none of the models showed high winds coming out eastward from the foothills, and thus, confidence in any winds moving into more populated areas and impacts was too low to include in the watch.

The day before (Wednesday 29 December) the Marshall Fire, available numerical models continued to show high winds remaining in the mountains and foothills east of the Continental Divide, including the first high-resolution model

runs from the HRRR and NAM-Nest models (both 3-km horizontal resolution). The High Wind Watch was upgraded to a High-Wind Warning, about 21 h before the start of the Marshall Fire, but given the uncertainty of how far east the high winds could reach, the lower elevations ( $<6000\text{ ft}$ ) were left out of the warning. Nevertheless, impact-based decision support services (IDSS; Uccellini and Ten Hoeve 2019) were provided to state and local emergency management officials, as well as the general public through social media and the NWS Boulder web page, all highlighting the potential for high winds from the higher elevations eastward to the Lyons–Boulder–Golden corridor. Given

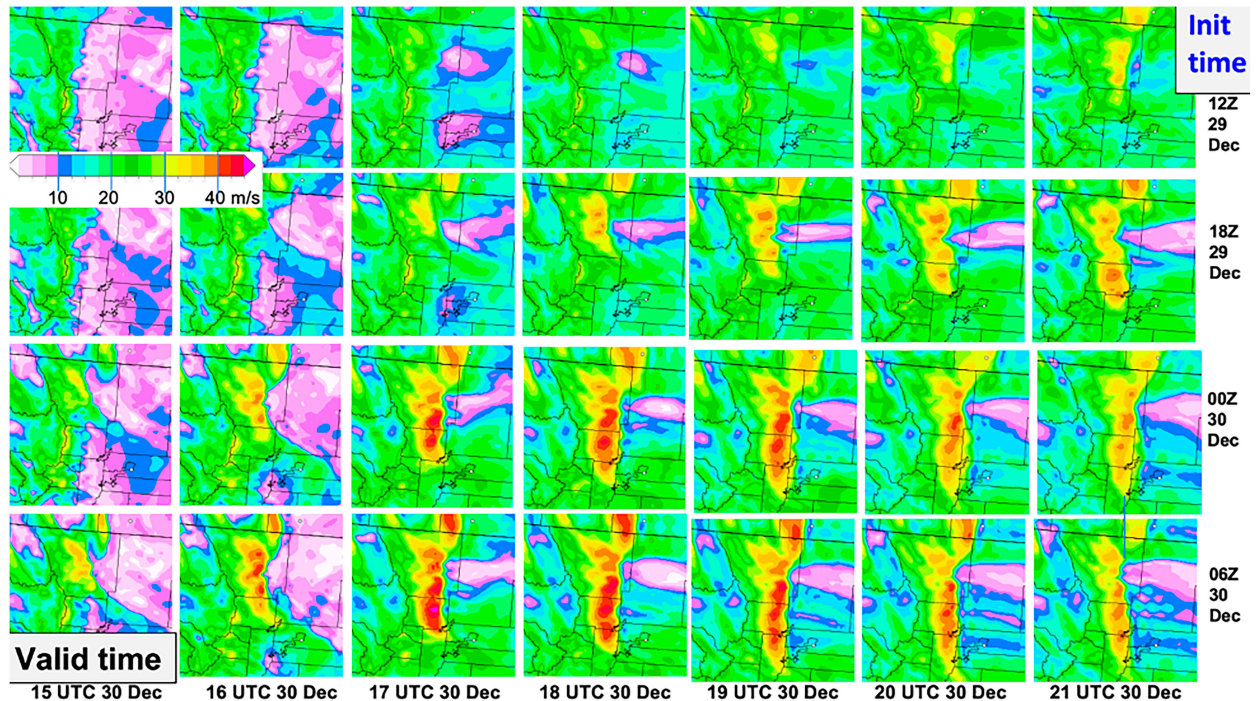


FIG. 19. Wind-gust potential fields ( $\text{m s}^{-1}$ ) from HRRR forecasts, now with matched valid times (shown in columns from left to right) from different initial times (in different rows, from older at top to more recent at bottom).

the extreme dryness of the fine fuels (mainly grasses) across the region, the high winds, and the expected 20%–30% relative humidity, fire danger was also highlighted as an additional impact for which to prepare.

As discussed previously, starting with the 0000 UTC 30 December HRRR run from Wednesday evening, strong mountain wave-induced downslope winds were consistently predicted in the Lyons–Boulder–Golden area and points 10–15 km to the

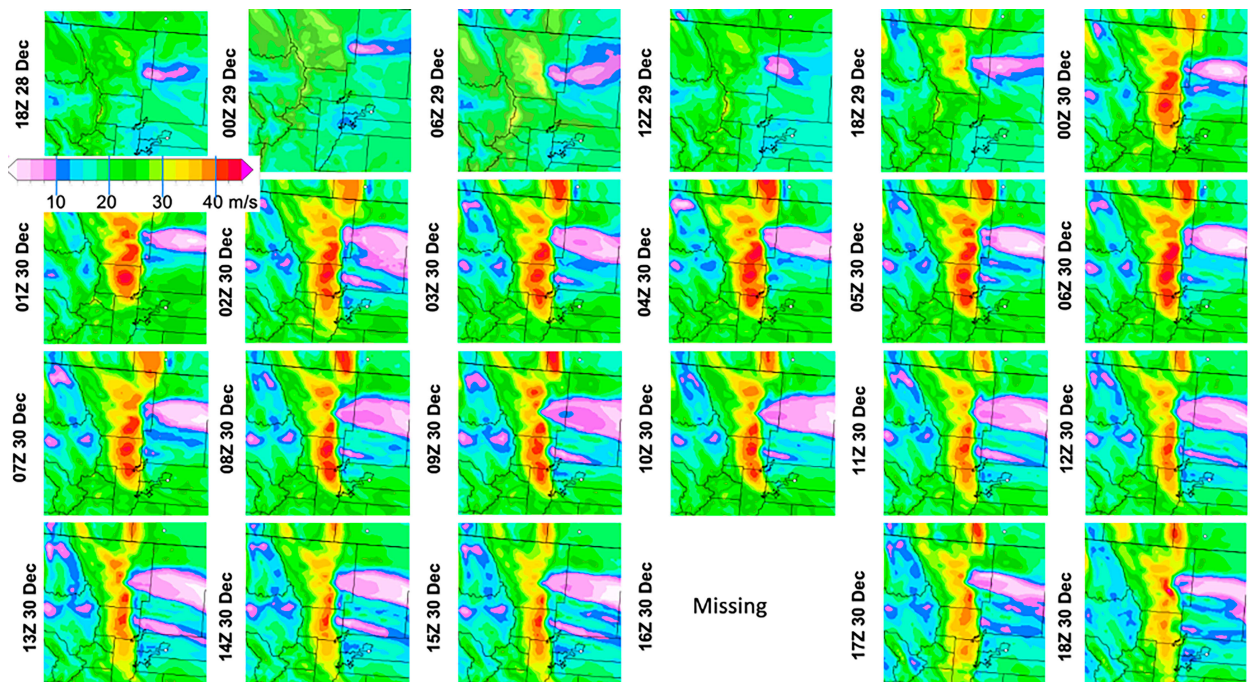


FIG. 20. Wind-gust potential ( $\text{m s}^{-1}$ ) forecasts from a series of HRRR model runs initialized at different times shown, all valid at 1800 UTC 30 Dec 2021.



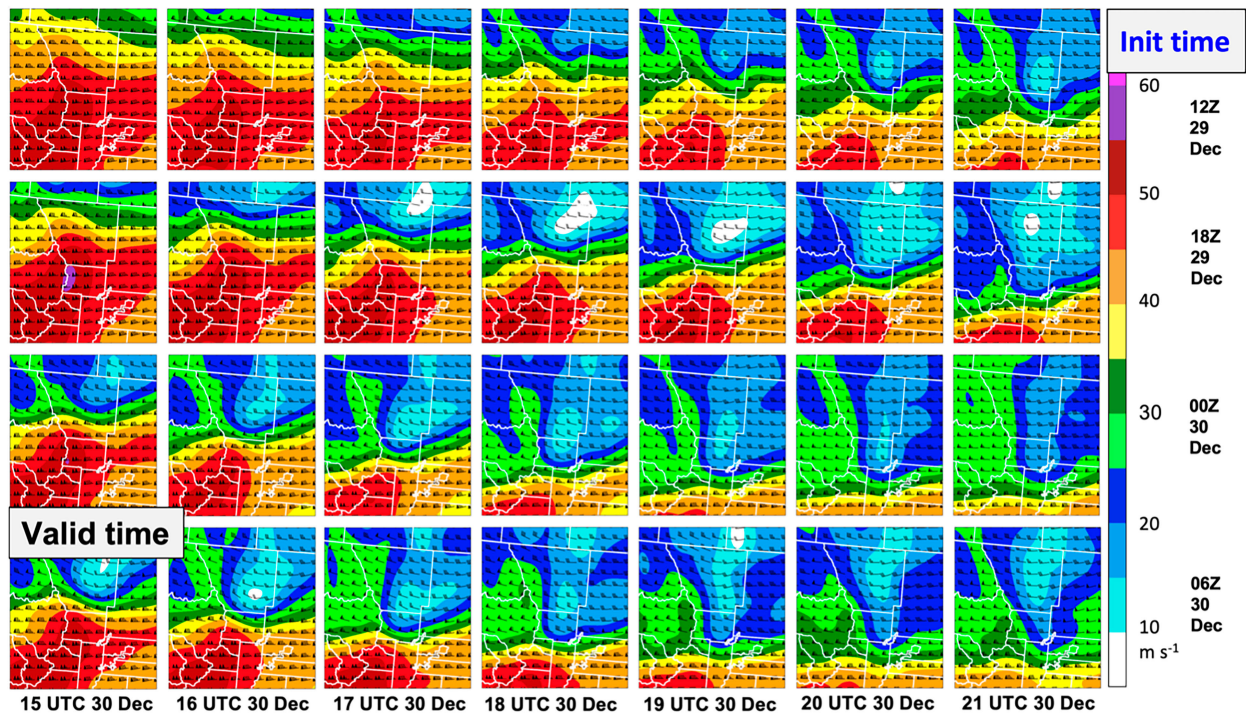


FIG. 21. The 400-hPa wind ( $\text{m s}^{-1}$ ) from HRRR forecasts, now with matched valid times from different initial times and corresponding to the same times shown for WGP in Fig. 19.

east. This is a typical occurrence in mountain waves, and the fact that every single hourly run of the HRRR predicted a high-wind event led the forecasters at NWS Boulder to issue a High-Wind Warning for the lower elevations below 6000 ft and adjacent plains of Larimer, Boulder, and Jefferson Counties at 0300 LT (1000 UTC) 30 December, roughly 5 h before the start of the high winds and 8 h before the Marshall Fire ignited. The decision support services also ramped up with renewed confidence in significant impacts across the lower elevations, highlighting the potential for wind damage and extreme fire behavior, especially once the Marshall Fire had been ignited. The High-Wind Warning for the city of Boulder triggered a countywide burn ban for Boulder County, which was in effect for 30 December. The consistency of the HRRR forecasts, as well as the model's ability to predict the overall trends in the evolution of the mountain wave, were the primary reasons the High-Wind Warning was issued for the adjacent plains along the Front Range. Forecasters at NWS Boulder incorporated experience and an understanding of the ingredients to augment the HRRR forecasts and generated a more accurate public forecast temporally and spatially prior to the Marshall Fire ignition.

While the forecast wind gusts were not precise in the exact subcounty areas where they occurred, forecasters generally do not focus on such detail in the model predictions, instead taking note of the consistent predictions of strong wind gusts reaching the plains adjacent to the Front Range. The WGP maximum values predicted for 30 December were higher than forecasters are accustomed to seeing from the HRRR, but the persistence of these strong gusts in so many consecutive hourly runs can

give them increasing confidence in their likelihood of verifying. In fact, it was indeed the run-to-run consistency in the hourly HRRR forecasts starting with the 0000 UTC 30 December run (Fig. 18, column 3) that was a significant factor in the issuance of the High-Wind Warning (HWW) to include the adjacent plains of Larimer, Boulder, and Jefferson Counties at 1000 UTC 30 December (Fig. 23). The NWS Area Forecast Discussion issued at 1000 UTC stated, “HRRR shows gusts up to 90 mph and has these winds spreading further east than some of the other Hi-Res data.” Forecasters also frequently analyze the HREF for downslope winds. Like the HRRR, the HREF showed high winds across the Lyons–Boulder–Golden corridor starting with the 0000 UTC 30 December 2021 model run, very much in line with the HRRR (not shown). This is not surprising as 2 of the 10 ensemble members of the HREF come from the HRRR itself (starting with HRRRv2.1). However, the HREF is only run every 12 h, limiting its role in the High-Wind Warning decision made the morning of 30 December 2021.

Forecasters in the NWS Forecast Office in Boulder are experienced with downslope winds, looking for ingredients to make the forecast and focusing on typical patterns. For example, when forecasters predict favorable ingredients for a strong mountain-wave event (e.g., 25–40  $\text{m s}^{-1}$  cross-barrier flow, a stable layer near mountain top (near 600 hPa), little wind shear at and above the inversion layer) along the Front Range, they know the strongest winds will be in a narrow corridor at the base of the foothills, west of Interstate 25, and generally along U.S.-36 from Lyons (northern Boulder County) to Boulder and Colorado State Highway 93 and then southward to Golden (Jefferson County).



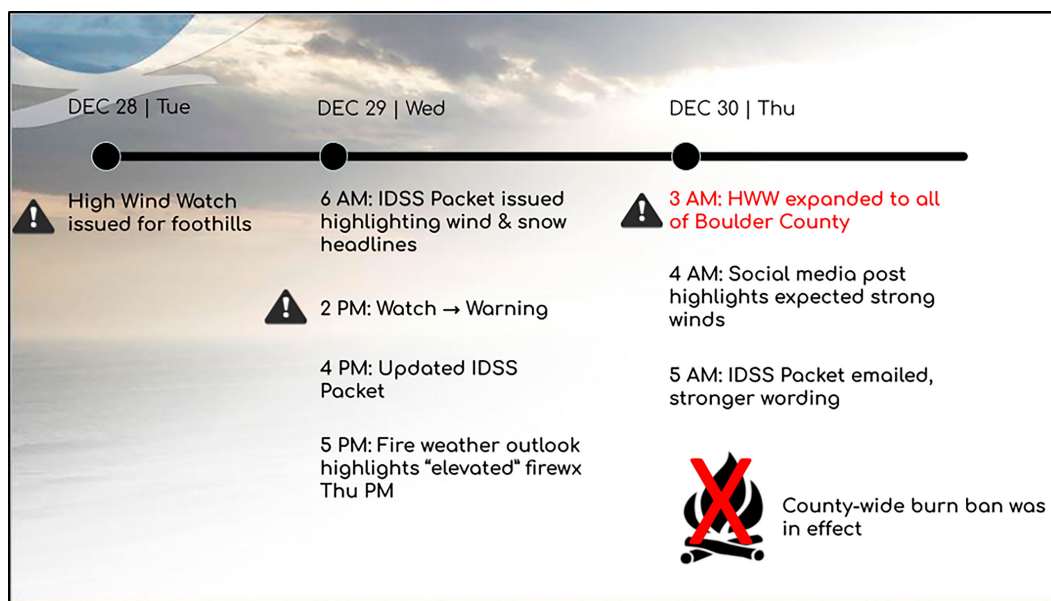


FIG. 22. Timeline of NWS bulletins for the 30 Dec 2021 event. IDSS: Impact-Based Decision Support Services. HWW: High-Wind Warning. Times are in local time (LT).

Both the NWS Forecast Office in Boulder and the Storm Prediction Center in Norman, Oklahoma, specifically mentioned in their routine products issued on 29 December that there would be a risk of elevated fire weather conditions across north-central

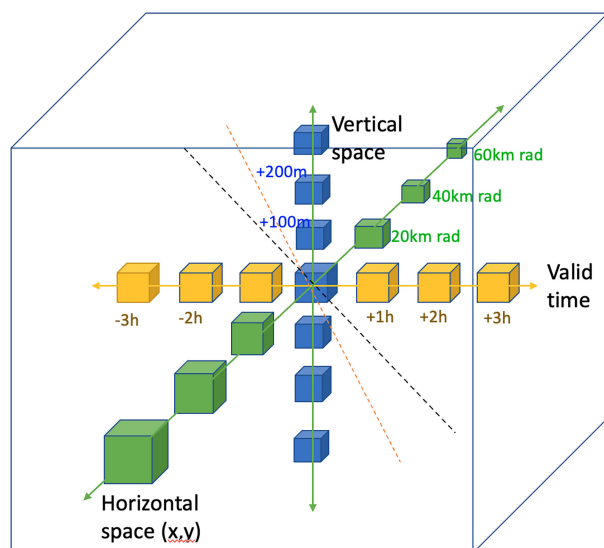


FIG. 23. Candidates for ensemble dimensions (applicable for a hazardous event): 1) different valid times (e.g., -2, -1, 0 +1, +2 h), 2) forecast initial time valid at same time (e.g., time-lagged, not shown), 3) ensemble members with the same initial time (not shown but the most common component of ensemble prediction), 4) horizontal space (x, y), 5) vertical space, 6) variable transformation, 7) other variables, and 8) variable range (values near to critical hazard value). Extra axes (dotted, dashed) nominally represent additional dimensions not explicitly shown in this diagram.

Colorado on 30 December. Although a HWW was issued for this event, a Red Flag Warning (RFW) was not issued since its relative humidity (RH) criterion<sup>2</sup> was not expected to be met. The predicted (and observed) 2-m RH in the fire area started at about 40% in morning hours of 30 December and decreased to 30% with 2-m temperature remaining at 5°–7°C. Given the favorable fuel environment, the 2-m RH combined with the extreme winds was clearly sufficient to allow rapid fire spread even though RH was well above the current RFW criterion of 15%. Observed RH was around 20%–28% near the fire, and down to 12%–15% at 25–30 km at one location east of the fire. As mentioned above, the HWW was sufficient to trigger the issuance of a countywide burn ban for 30 December early that morning. The conditions documented in this paper for the Marshall windstorm suggest that the RH criterion should be substantially relaxed especially given the extreme winds, possibly as part of a redesign of RFW criteria. Lindley et al. (2011), Jolly et al. (2019), Clark et al. (2020), and Jakober et al. (2023) all address the fact that impactful wildfires occur along a spectrum of conditions that is not limited to currently defined RFW criteria, as was the case with the Marshall Fire. While it is unknown whether an RFW may have impacted the decision-making on 30 December 2021, we recommend that the RFW should be modernized to fit the needs of both fire managers and the general public in light of major recent fires like the Marshall Fire that may not have met the local criteria for an RFW.

The NWS Forecast Office in Boulder used social media to message potential impacts from the high winds, and once the fire started, they issued life-saving tweets and Facebook posts to amplify evacuation messages and help residents of eastern

<sup>2</sup> NWS Red Flag Warning criteria as of August 2023: <https://www.weather.gov/gjt/firewxcriteria>, including 15% RH for Colorado.

Boulder County understand their risk. Official Spot Weather forecasts (e.g., like those requested from and delivered to <https://www.weather.gov/spot>) are a critical tool for emergency management officials including first responders in the fire and police communities. The NWS Forecast Office in Boulder provided Spot Weather forecasts twice per day from 30 December 2021 to 7 January 2022. Frequent briefings with emergency management officials during the fire provided critical local level forecasts necessary for first-responder safety and resource mobilization, and these occurred roughly every hour from shortly after ignition through the evening of 30 December. Having a consistent HRRR forecast depicting where the strongest winds would occur, and how long they would continue, was a critical part of effective messaging in life-or-death situations with this rapidly growing fire.

#### *Discussion on ensemble dimensions used in this study*

In this paper, we have explored a range of different perspectives of forecasts for the Colorado Front Range windstorm that quickly drove the Marshall Fire into the wildland–urban interface. Rather than simply examining forecasts of 10-m wind speed, we examined forecasts of wind-gust potential (with assumptions about boundary layer mixing) and the vertical dimension of horizontal wind (representing to whatever extent a classical downslope wind structure). Moreover, we have also examined forecasts valid throughout the 12-h period from 1200 to 0000 UTC Thursday 30 December 2021. Using a combination of vertical wind structure and a matrix of valid times, we were able to show an indication of an extreme wind event ( $>30 \text{ m s}^{-1}$  sustained wind within 200–400 m of the surface) from HRRR forecasts as early as that initialized at 1200 UTC Wednesday 29 December 2021 (Fig. 18).

Quantification of uncertainty is a key component of predicting an extreme event. Probabilistic forecasts can be derived from model ensembles; convection-allowing model (CAM) ensembles (e.g., Clark et al. 2021; Demuth et al. 2020), which allow explicit representation of rotating thunderstorms, have allowed direct probability forecasts of explicit severe convective events (e.g., strong updraft helicity, hail, severe wind gusts). CAM ensembles can also be used for other small-scale significant weather events, including extreme convective rain events, mesoscale snowbands, coastal sea/lake breezes, and others. The only operational CAM ensemble in the United States is HREF (Clark et al. 2021), which is not a formal ensemble but rather a combination of different available models and initialization times. However, the diversity of models and dynamical cores and 12-h update frequency in the HREF poses challenges for predicting some phenomena.

Questions for operational forecasters for this event were 1) what kind of windstorm event might occur, if any, 2) was there a potential for an extreme wind event warranting a High-Wind Warning east of the Front Range foothills, and 3) what can the NWS do to improve the warning process for fire weather partners and the public when facing sub-RFW weather conditions similar to what occurred on 30 December 2021 in Colorado? A range of ensemble dimensions (1–8) were considered here in this paper to revisit possible answers to the first two forecaster questions, and this range of dimensions is nominally depicted in Fig. 23. Question 3 is a much broader conversation for the fire weather enterprise.

A key message from this study is that, even in the absence of formal or ad hoc ensemble systems, consideration of spatial and temporal neighborhoods, as well as time-lagging of subsequent initializations, can provide probabilistic guidance on the likelihood of an extreme event from deterministic CAMs such as the HRRR. A temporal neighborhood includes a range of neighboring valid times to see if an event was forecast to occur during a wider forecast period (dimension 1 in Fig. 23). Consideration of multiple time-lagged initializations examines forecasts for trends or consistency (dimension 2). In the Marshall Fire case, consistency of hourly initialized HRRR forecasts starting at 0000 UTC 30 December 2021 was important for the issuance of the High-Wind Warning for the lower elevations of Boulder County after 0800 UTC.

Probabilistic predictions based on deterministic CAMs should also take advantage of spatial neighborhoods, in both the horizontal and vertical (dimensions 4 and 5). The horizontal neighborhood allows for the fact that a deterministic CAM prediction may have some displacement error in the location of a relevant feature (e.g., a convective storm, or latitudinal position of a zonal downslope windstorm). It is appropriate to take into account this uncertainty by considering predictions over both spatial and temporal neighborhoods, as demonstrated by Sobash et al. (2020) for their neural network for predicting severe convective storms. The vertical neighborhood allows for some vertical displacement in a deterministic CAM prediction of a relevant feature, such as a subsidence inversion, and could also be used in a machine learning approach.

Finally, transformations (dimension 6) such as the WGP diagnosis can be applied, operating on formal or time-lagged ensemble members with, for example, slightly different surface  $\theta_s$ , to examine sensitivity to boundary layer structure. Similarly, machine learning can use environmental and storm attribute predictors (dimension 7 or extend critical value range (dimension 8) to provide further probabilistic information beyond explicit prediction of phenomena by CAM forecasts, as shown by Herman and Schumacher (2018).

## 6. Conclusions

The 30 December 2021 Boulder County downslope windstorm in Colorado led to rapid spread of fires, most importantly, the Marshall Fire. This was a catastrophic urban fire event dependent on persistent extreme near-surface winds. Wind gusts of at least  $35 \text{ m s}^{-1}$  began at 1500 UTC that day, but fire ignition(s) did not occur until after 1800 UTC when wind gusts increased to  $45\text{--}50 \text{ m s}^{-1}$ . Outlooks for a strong wind event in the foothills on 30 December were issued 2 days earlier on 28 December. The NWS was then aware of the threat for a windstorm on the plains at lower elevation than the foothills, and its challenge was when or whether to issue an urban ( $<6000 \text{ ft}$ ) High Wind Watch or Warning.

The windstorm prediction, shown through this study, was dependent on large-scale dynamics and the exact location and timing for a northward shift of the large-scale cross-continent upper-level jet axis with west-to-southwesterly flow between 0000 and 1200 UTC the evening before and then a subsequent southward shift after 1200 UTC 30 December 2021. The

southward shift was also reflected in hourly observed and analyzed 10-m wind gusts and observed pressure traces from Cheyenne, Wyoming, through Boulder County into Jefferson County. The evolution of the event was examined from a three-dimensional perspective with fields from the surface, aloft, and with vertical cross sections linking different levels and allowing comparison with a classical downslope windstorm structure. This windstorm varied from typical Boulder downslope windstorms in the role of this westerly jet [no northwest wave as in Mercer et al. (2008)], the duration of the event (~11 h), the absence of either warm- or cold-air advection (neither chinook nor bora), and the peculiar southwest direction of surface wind in Boulder (not the typical 270°–290° direction).

A review was described of the NWS operational process considering the possibility of a windstorm and then with issuance of a High Wind Watch and then, of an urban High-Wind Warning linking forecaster decisions with the NWP guidance. (We recommend revision of RFW criteria as discussed in section 5.) Run-to-run consistency of hourly HRRR forecasts starting at 0000 UTC 30 December was critical for issuance of this warning. Subsequent HRRR forecasts, once the fire initiated, were key when providing IDSS to emergency officials. We note that extending hourly CAM predictions to 24 h or longer would allow inspection of this run-to-run consistency from 18 to 24 h before the possible event rather than using the 12–18-h forecasts dictated by current HRRR hourly forecast duration of 18 h. Details of downslope storm prediction are highly dependent on fine differences in initial conditions (e.g., Reinecke and Durran 2009). We finally showed how eight different ensemble dimensions could be combined to consider the possibility of an extreme urban high-wind event, several of which were used in this study. These dimensions included both temporal and spatial aggregations which should be added to ensembles for extreme weather events. Our examination of the Marshall Fire event in this context illustrates how probabilistic information can be obtained from a frequently updated deterministic CAM. We hope this summary provides helpful insights on predictions of severe downslope wind events and on effective forecaster–modeler collaboration on such studies.

**Acknowledgments.** We thank David Barjenbruch (NWS Boulder) and Trevor Alcott (GSL) for extremely helpful internal reviews. We express thanks also to Todd Lindley (NWS Norman), two anonymous reviewers, and the editor for excellent reviews leading to important improvements.

**Data availability statement.** HRRR data are publicly available via archives hosted by Amazon Web Services (<https://registry.opendata.aws/noaa-hrrr-pds/>) and Google Cloud Platform (<https://console.cloud.google.com/marketplace/product/noaa-public/hrrr?project=python-232920&pli=1>).

## REFERENCES

- Benjamin, S. G., and Coauthors, 2016: A North American hourly assimilation and model forecast cycle: The Rapid Refresh. *Mon. Wea. Rev.*, **144**, 1669–1694, <https://doi.org/10.1175/MWR-D-15-0242.1>.
- , E. P. James, J. M. Brown, E. J. Szoke, J. S. Kenyon, R. Ahmadov, and D. D. Turner, 2021: Diagnostic fields developed for hourly updated NOAA weather models. NOAA Tech. Memo. OAR GSL-66, 55 pp., <https://doi.org/10.25923/f7b4-rx42>.
- Boulder County, 2022: Marshall Fire operational After-Action Report (AAR). Marshall Fire After Action Rep., 55 pp., <https://assets.bouldercounty.gov/wp-content/uploads/2022/06/marshall-fire-after-action-report.pdf>.
- , 2023: Boulder County Wildfire History Story Map. Accessed 2 May 2023, <https://bouldercounty.gov/disasters/wildfires/maps-and-videos/>; Map shown in <https://bouldercounty.maps.arcgis.com/apps/MapJournal/index.html?appid=9ceb4d1c33274c88af2aad5abf77bcb>.
- Boulder County Sheriff's Office, 2023: Marshall Fire investigative summary and review. Boulder County Sheriff's Office, 18 pp., <https://assets.bouldercounty.gov/wp-content/uploads/2023/06/marshall-fire-investigative-summary.pdf>.
- Brinkmann, W. A. R., 1973: A climatological study of strong downslope winds in the Boulder area. NCAR Cooperative Thesis 27, INSTAAR Occasional Paper 7, 250 pp., <https://www.colorado.edu/instaar/sites/default/files/attached-files/OP07-Brinkmann-1973.pdf>.
- , 1974: Strong downslope winds at Boulder, Colorado. *Mon. Wea. Rev.*, **102**, 592–602, [https://doi.org/10.1175/1520-0493\(1974\)102<0592:SDWABC>2.0.CO;2](https://doi.org/10.1175/1520-0493(1974)102<0592:SDWABC>2.0.CO;2).
- Clark, A. J., and Coauthors, 2021: A real-time, virtual spring forecasting experiment to advance severe weather prediction. *Bull. Amer. Meteor. Soc.*, **102**, E814–E816, <https://doi.org/10.1175/BAMS-D-20-0268.1>.
- Clark, J., J. T. Abatzoglou, N. J. Nauslar, and A. M. S. Smith, 2020: Verification of red flag warnings across the northwestern U.S. as forecasts of large fire occurrences. *Fire*, **3**, 60, <https://doi.org/10.3390/fire3040060>.
- Colorado Department of Natural Resources, 2018: Colorado underground coal mine fires. 2018 Inventory Rep., Colorado Department of Natural Resources, 254 pp., <http://hermes.cde.state.co.us/drupal/islandora/object/co:35359/datastream/OBJ/view>.
- Colorado Division of Fire Prevention and Control, 2022: News release: Marshall Fire facilitated learning analysis. Colorado Division of Fire Prevention and Control, accessed 15 September 2023, <https://dfpc.colorado.gov/MarshallFireFLA>.
- Demuth, J. L., and Coauthors, 2020: Recommendations for developing useful and usable convection-allowing model ensemble information for NWS forecasters. *Wea. Forecasting*, **35**, 1381–1406, <https://doi.org/10.1175/WAF-D-19-0108.1>.
- Dowell, D. C., and Coauthors, 2022: The High-Resolution Rapid Refresh (HRRR): An hourly updating convection-allowing forecast model. Part I: Motivation and system description. *Wea. Forecasting*, **37**, 1371–1395, <https://doi.org/10.1175/WAF-D-21-0151.1>.
- Durran, D. R., 1986: Another look at downslope windstorms. Part I: The development of analogs to supercritical flow in an infinitely deep, continuously stratified fluid. *J. Atmos. Sci.*, **43**, 2527–2543, [https://doi.org/10.1175/1520-0469\(1986\)043<2527:ALADWP>2.0.CO;2](https://doi.org/10.1175/1520-0469(1986)043<2527:ALADWP>2.0.CO;2).
- , 1990: Mountain waves and downslope winds. *Atmospheric Processes over Complex Terrain*, W. Blumen, Ed., Amer. Meteor. Soc., 59–81.



- , and J. B. Klemp, 1983: A compressible model for the simulation of moist mountain waves. *Mon. Wea. Rev.*, **111**, 2341–2361, [https://doi.org/10.1175/1520-0493\(1983\)111<2341:ACMFTS>2.0.CO;2](https://doi.org/10.1175/1520-0493(1983)111<2341:ACMFTS>2.0.CO;2).
- Fovell, R. G., and A. Gallagher, 2022: An evaluation of surface wind and gust forecasts from the High-Resolution Rapid Refresh model. *Wea. Forecasting*, **37**, 1049–1068, <https://doi.org/10.1175/WAF-D-21-0176.1>.
- , M. J. Brewer, and R. J. Garmon, 2022: The December 2021 Marshall Fire: Predictability and gust forecasts from operational models. *Atmosphere*, **13**, 765, <https://doi.org/10.3390/atmos13050765>.
- Herman, G. R., and R. S. Schumacher, 2018: Money doesn't grow on trees, but forecasts do: Forecasting extreme precipitation with random forests. *Mon. Wea. Rev.*, **146**, 1571–1600, <https://doi.org/10.1175/MWR-D-17-0250.1>.
- Jakober, S., T. Brown, and T. Wall, 2023: Development of a decision matrix for National Weather Service red flag warnings. *Fire*, **6**, 168, <https://doi.org/10.3390/fire6040168>.
- James, E. P., S. G. Benjamin, and B. D. Jamison, 2020: Commercial aircraft-based observations for NWP: Global coverage, data impacts, and COVID-19. *J. Appl. Meteor. Climatol.*, **59**, 1809–1825, <https://doi.org/10.1175/JAMC-D-20-0010.1>.
- , and Coauthors, 2022: The High-Resolution Rapid Refresh (HRRR): An hourly updating convection-allowing forecast model. Part II: Forecast performance. *Wea. Forecasting*, **37**, 1397–1417, <https://doi.org/10.1175/WAF-D-21-0130.1>.
- Jolly, W. M., P. H. Freeborn, W. G. Page, and B. W. Butler, 2019: Severe fire danger index: A forecastable metric to inform firefighter and community wildfire risk management. *Fire*, **2**, 47, <https://doi.org/10.3390/fire2030047>.
- Juliano, T. W., and Coauthors, 2023: Toward a better understanding of wildfire behavior in the wildland-urban interface: A case study of the 2021 Marshall Fire. *Geophys. Res. Lett.*, **50**, e2022GL101557, <https://doi.org/10.1029/2022GL101557>.
- Kuenzer, C., and G. B. Stracher, 2012: Geomorphology of coal seam fires. *Geomorphology*, **138**, 209–222, <https://doi.org/10.1016/j.geomorph.2011.09.004>.
- Lilly, D. K., 1978: A severe downslope windstorm and aircraft turbulence event induced by a mountain wave. *J. Atmos. Sci.*, **35**, 59–77, [https://doi.org/10.1175/1520-0469\(1978\)035<0059:ASDWAA>2.0.CO;2](https://doi.org/10.1175/1520-0469(1978)035<0059:ASDWAA>2.0.CO;2).
- , and E. J. Zipser, 1972: The front range windstorm of 11 January 1972: A meteorological narrative. *Weatherwise*, **25**, 56–63, <https://doi.org/10.1080/00431672.1972.9931577>.
- Lindley, T. T., J. D. Vitale, W. S. Burgett, and M.-J. Beierle, 2011: Proximity meteorological observations for wind-driven grassland wildfire starts on the Southern Great Plains. *Electron. J. Severe Storms Meteor.*, **6** (1), <https://ejssm.org/archives/2011/vol-6-1-2011/>.
- Lu, W., Y.-J. Cao, and J. C. Tien, 2017: Method for prevention and control of spontaneous combustion of coal seam and its application in mining field. *Int. J. Min. Sci. Technol.*, **27**, 839–846, <https://doi.org/10.1016/j.ijmst.2017.07.018>.
- Mercer, A. E., M. B. Richman, H. B. Bluestein, and J. M. Brown, 2008: Statistical modeling of downslope windstorms in Boulder, Colorado. *Wea. Forecasting*, **23**, 1176–1194, <https://doi.org/10.1175/2008WAF2007067.1>.
- National Weather Service, 2021: Factors on wildfire today. NWS Boulder, accessed 15 April 2023, [https://twitter.com/NWSBoulder/status/1476803594196193280?ref\\_src=twsrc%5Etfw%7Ctwcamp%5Etweetembed%7Ctwterm%5E1476803594196193280%7Ctwgr%5E275a85511f590575e018e952be18dcb52d3e23d4%7Ctwcon%5Es1\\_&ref\\_url=https%3A%2F%2Fwww.denver7.com%2Fnews%2Fmarshall-fire%2Fnational-weather-service-analysis-identifies-factors-that-caused-marshall-fire-to-spread-so-quickly](https://twitter.com/NWSBoulder/status/1476803594196193280?ref_src=twsrc%5Etfw%7Ctwcamp%5Etweetembed%7Ctwterm%5E1476803594196193280%7Ctwgr%5E275a85511f590575e018e952be18dcb52d3e23d4%7Ctwcon%5Es1_&ref_url=https%3A%2F%2Fwww.denver7.com%2Fnews%2Fmarshall-fire%2Fnational-weather-service-analysis-identifies-factors-that-caused-marshall-fire-to-spread-so-quickly).
- NOAA/Physical Science Laboratory, 2023: Boulder wind info. Accessed 10 May 2023, <https://psl.noaa.gov/boulder/wind.html#windtable>.
- Reinecke, P. A., and D. R. Durran, 2009: Initial-condition sensitivities and the predictability of downslope winds. *J. Atmos. Sci.*, **66**, 3401–3418, <https://doi.org/10.1175/2009JAS3023.1>.
- RMIIA, 2023: Colorado wildfire information. Accessed 15 April 2023, [http://www.rmiiia.org/catastrophes\\_and\\_statistics/Wildfire.asp](http://www.rmiiia.org/catastrophes_and_statistics/Wildfire.asp).
- Sangster, W. E., 1972: An objective forecast technique for Colorado downslope winds. NOAA Tech. Memo. NWS CR-50, 30 pp., [https://repository.library.noaa.gov/view/noaa/30362/noaa\\_30362\\_DS1.pdf](https://repository.library.noaa.gov/view/noaa/30362/noaa_30362_DS1.pdf).
- Smith, R. B., 2019: 100 years of progress in mountain meteorology research. *A Century of Progress in Atmospheric and Related Sciences: Celebrating the American Meteorological Society Centennial*, Meteor. Monogr., No. 59, Amer. Meteor. Soc., <https://doi.org/10.1175/AMSMONOGRAPHS-D-18-0022.1>.
- Sobash, R. A., G. S. Romine, and C. S. Schwartz, 2020: A comparison of neural-network and surrogate-severe probabilistic convective hazard guidance derived from a convection-allowing model. *Wea. Forecasting*, **35**, 1981–2000, <https://doi.org/10.1175/WAF-D-20-0036.1>.
- Uccellini, L. W., and D. R. Johnson, 1979: The coupling of upper and lower tropospheric jet streaks and implications for the development of severe convective storms. *Mon. Wea. Rev.*, **107**, 682–703, [https://doi.org/10.1175/1520-0493\(1979\)107<0682:TCOUAL>2.0.CO;2](https://doi.org/10.1175/1520-0493(1979)107<0682:TCOUAL>2.0.CO;2).
- , and J. E. Ten Hoeve, 2019: Evolving the National Weather Service to build a Weather-Ready Nation: Connecting observations, forecasts, and warnings to decision-makers through impact-based decision support services. *Bull. Amer. Meteor. Soc.*, **100**, 1923–1942, <https://doi.org/10.1175/BAMS-D-18-0159.1>.